DOKUZ EYLÜL UNIVERSITY
GRADUATE SCHOOL OF NATURAL AND APPLIED SCIENCE

IMPACT RESPONSE OF RAMOR500 ARMOR STEEL SUBJECTED TO HIGH VELOCITIES

by
İlker MEMİŞ

October, 2016
İZMİR

IMPACT RESPONSE OF RAMOR500 ARMOR STEEL SUBJECTED TO HIGH VELOCITIES

A Thesis Submitted to the
Graduate School of Natural and Applied Science of Dokuz Eylül University
In Partial Fullfilment of the Requirements for the Master of Science of
Mechanical Engineering, Mechanic Program

by
İlker MEMİŞ

October, 2016
İZMİR

M.Sc THESIS EXAMINATION RESULT FORM

We have read the thesis entitled **"IMPACT RESPONSE OF RAMOR500 ARMOR STEEL SUBJECTED TO HIGH VELOCITIES"** completed by **İLKER MEMİŞ** under supervision of **PROF. DR. RAMAZAN KARAKUZU** and we certify that in our opinion it is fully adequate, in scope and in quality, as a thesis for the degree of Master of Science.

Prof. Dr. Ramazan KARAKUZU

Supervisor

Assoc. Prof. Dr. Yusuf ARMAN

(Jury Member)

Assis. Prof. Dr. Levent AYDIN

(Jury Member)

Prof.Dr. Emine İlknur CÖCEN
Director
Graduate School of Natural and Applied Sciences

ACKNOWLEDGEMENTS

I would like to thank to my commiter chair, Prof. Ramazan KARAKUZU for leading and helping me during my thesis. I would also like to thank to Dr. Ali KARA at I.Y.T.E. for supporting me with theoretical knowledges, thank to Research Assistant Volkan ARIKAN for helping me during my experimental works, thank to R&D Manager Aydın AKYÜZ from Katmerciler A.Ş. for supplying me specimens and photos, thank to Mr. Uğur who is the testing supervisor at polygon in Çiçekliköy for helping me during all my shooting tests.

In addition, I would like to express my deepest appreciation to my family for their prayer and moral support.

İlker MEMİŞ

IMPACT RESPONSE OF RAMOR500 ARMOR STEEL SUBJECTED TO HIGH VELOCITIES

ABSTRACT

Ballistic is a science that includes investigation of behaviour of projectiles on targets. By the developing of technology, the result of combination of theoretical knowledge with the software, the complex problems become solved by simple methods. That's why, the critical experimental methods in defense industry can be solved by special programs in a short time.

In this study, Ramor500 armor steel which is used for protection at TOMA (Anti-Riot Vehicle) was tested for relevance of NIJ LEVEL IIIA, experimentally and numerically by computer. For this purpose, the steel specimen with dimensions of 500x500x3 mm was shot by 9 mm Parbellum projectile for three times at the reliable polygon and deformations are photographed. On the other hand, the mechanical properties of specimens were found by tensile test at different temperature and The Johnson-Cook (J-C) parameters were obtained by using Hopkinson-Split Bar test data. By using these data the same shooting test was simulated on ANSYS Explicit Dynamic module. In this way, it is realized that experimental and simulation results were good agreement. In addition, the puncture thickness of Ramor500 at the constant projectile velocity and the puncture velocity at the constant thickness were obtained by using ANSYS Explicit Dynamic.

Keywords: Ramor500, armor steel, TOMA, ballistic, FMJ, impact response, NIJ LEVEL.

YÜKSEK HIZLARA MARUZ RAMOR500 ZIRH ÇELİĞİNİN DARBE CEVABI

ÖZ

Balistik, mermilerin hedef üzerindeki davranışını inceleyen bir bilim dalıdır. Gelişen teknoloji ile birlikte teorik altyapının yazılımla birleşmesi sonucu karmaşık problemler basit yöntemlerle çözülür hale gelmiştir. Bu sebeple savunma sanayisinde kritik öneme sahip deneysel yöntemler artık özel programlar sayesinde kısa süre içerisinde çözülebilmektedir.

Bu çalışmada TOMA araçlarında zırhlama amacıyla kullanılan Ramor500 çeliğinin NIJ LEVEL IIIA standardına uygunluğu deneysel ve bilgisayar ortamında nümerik olarak test edilmiştir. Bu amaçla 500x500x3 mm ebatlarındaki çelik numunesine güvenlik önlemleri alınmış atış poligonunda 5 m mesafeden 9mm Parabellum mermi ile 3 el atış yapılmış, oluşan deformasyonlar kayıt altına alınmıştır. Diğer yandan aynı çeliğe ait çeki testi numunesi farklı sıcaklıklarda çekilerek mekanik özellikleri bulunmuş ve Hopkinson-Split Bar testi yardımıyla Johnson-Cook (J-C) parametreleri elde edilmiştir. Bu parametreler yardımıyla aynı atış testi ANSYS Explicit Dynamic modülünde simule edilmiştir. Bu sayede gerçek şartlarda elde edilen sonuçlarla simülasyon sonuçlarının birbirine yakın olduğu görülmüştür. Ayrıca Ramor500 zırh çeliğinin sabit atış hızında delinebildiği kalınlık ve sabit kalınlıkta delinebildiği hız miktarı da ANSYS Explicit Dynamic yardımıyla tayin edilmiştir.

Anahtar kelimeler: Ramor500, zırh çeliği, TOMA, balistik, FMJ, darbe cevabı, NIJ LEVEL.

CONTENTS

Page

LIST OF FIGURES

Page

LIST OF TABLES

Page

CHAPTER ONE
INTRODUCTION

Ballistic is a science that includes investigation of behaviour of projectiles on targets. By the developing of technology, the result of combination of theoretical knowledge with the software, the complex problems become solved by simple methods. That's why, the critical experimental methods in defense industry can be solved by special programs in a short time.

TOMA (Intervention Vehicle to Social Events or Anti Riot Vehicle) is an armored truck designed for requirements of police department and military. It is also used by lots of countries for various function such as preventing riots or fire fighting.

Different type of powered trucks are used for production of TOMA and always used the newest model. TOMA has 30% gradient climbing capability. The critical sub-systems of TOMA such as cabin, fuel tank, air tank, batteries are also protected against ballistic threat. On the other hand, TOMA has self-extinguishing system against flammable stuff such as molotov cocktail etc. The weight of TOMA is changeable due to the capacity of water tank. The water tank capacity can be changed range of 5 to 15 tonnes.

Figure 1.1 Mercedes Atego 1829K 4x2 TOMA (Ürünlerimiz, n.d.)

Bhat (2007) investigated the impact response of ballistic applications. Hybrid-Composite-Armor (HCA) is a kind of sandwich structure was chosen for this study. Firstly, anisotropic properties were obtained via quasi-static compressing test. Secondly, SHPB test method was used for dynamic properties. After finding mechanical properties of the material ballistic test was performed. All methods were also used for 4130 steel plates. ABAQUS 6.8.2 and LS-DYNA was used for FEA modelling. It was found that simulation results were similar to experimental results.

Kıranlı (2009) worked on determination of constitutive equation of a biomedical grade Ti6A14V alloy for cross-wedge rolling. For this purpose, Johnson-Cook parameters were obtained by using SHPB. While SHPB testing, it was realized that yield stress increases with the increasing strain rate. In addition, the effect of temperature was observed on yield stress. After finding all parameters, they were compared with the literature. All of parameters are well agreed except compression tests.

Shrat, & Baker (2011) tried to describe the plastic behaviour of material by using Johnson-Cook model. The parameters of Johnson-Cook model were determined by curve fitting techniques. The aim of the study is re-identify Johnson-Cook parameters by using Levenberg-Morquardt technique.

Šlais, Dohnal & Forejt (2012) studied to compare between experiment and computer simulation of Ti6Al4V. Ansys LS-DYNA 3D program was used for simulation. The specimens were deformed at high strain rate using the device for the Taylor anvil test. After determination of Johnson-Cook parameters, good agreements were determined between experimental and simulation results.

Karagöz & Atapek (2007) studied to compare microstructural characteristic and test results of boron added steels that after applied different heat treatment. In addition, rupture characteristic was determined of fracture surfaces after impact test. After impact test, it was realized that the microstructure of new designed hardened

and tempered steel is pretty homogeneous. On the other hand, the results of impact tests presented satisfying characteristic.

Demircioğlu, & Candan, & Ay (2011) investigated the impact response of Kevlar and St-37 sheet material using 9 mm projectile. Ballistic standart was chosen as NIJ and the simulation program was AUTODYN. Steinberg Guinan model was used for the projectile and Johnson-Cook plasticity model was used for St-37. Equation of State (EOS) was used for Kevlar. All experimental and numerical simulation results were compared and were obtained a good agreement.

Candan (2007) investigated the impact response of high density polythene (UHMW-PE) armour plaque which were pressed and unpressed. In this study, only experimental methods were examined. It was realized that pressed plaque was more resistant than unpressed plaque.

In this study, the impact response of Ramor500 armor steel will be investigated by experimentally and numerically by using ANSYS Explicit Dynamic. First of all, Ramor500 will be shot for relevance of NIJ LEVEL IIIA. After experimental process, Johnson-Cook parameters will be studied to obtain by using quasi-static and SHPB tests. By using these parameters, impact responce of J-C model will be simulated by ANSYS Explicit Dynamic. Finally, experimental and simulated results will be compared.

On the other hand, the puncture thickness of Ramor500 at the constant projectile velocity and the puncture velocity at the constant thickness will be obtained by using ANSYS Explicit Dynamic.

CHAPTER TWO
BALLISTIC IMPACT BACKGROUND

2.1 Energy Absorption

Ballistic impact theory related to energy absorption. The main aim of energy absorption is prevention constructions from damage.

Energy absorption is a system that can convert the kinetic energy in any other form. Energy converted is reversible like elastic strain energy or irreversible like plastic deformation energy. In such cases, an irreversible mode of conversion is utilized more predominantly as it positively ensures that damages sustained through intense impact loads are minimal. Consequently, energy absorbers use elastic strain and plastic deformation energy as absorption, but plastic deformation energy is more influential than elastic strain energy for absorption.

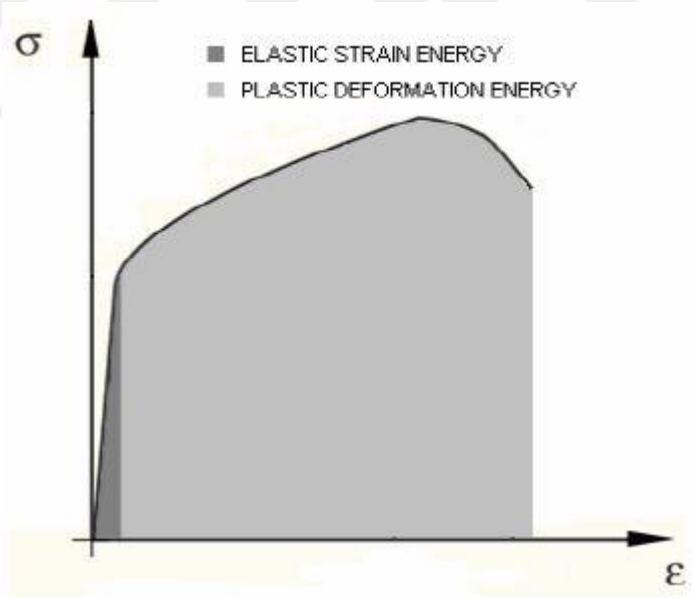

Figure 2.1 Elastic and plastic regions on a stress-strain diagram (Bhat, 2007)

Material properties play a vital role in governing the energy absorption capacities. For instance, metal alloys are better than aluminum alloys and ceramics in energy absorption. Ceramics have been used in ballistic armor applications due to their high compressive strength and low density. However, their use is limited to only specific

applications due to their brittle behavior. Metal alloys have been more useful in terms of manufacturing technology. High strength and low brittleness made metal alloys better than ceramics in energy absorption.

2.2 History of Ballistic Materials

While World War II, human life in combat zone started to become more important role. With the development of new weapon systems, it was needed to renovate the older armor technology to improve human and vehicle protection and invented Dual Hardness Armor (DHA), Rolled Homogenous Armor (RHA), Cast Homogenous Armor (CHA), High Hardness steel Armor (HHA), and hardened aluminum alloy armor. To improvement of performance, study of penetration mechanism gained attention. With developing of terminal ballistic, the characteristics and fragmentation of projectiles were started to investigate.

Figure 2.1 shows development of armor system performances by time.

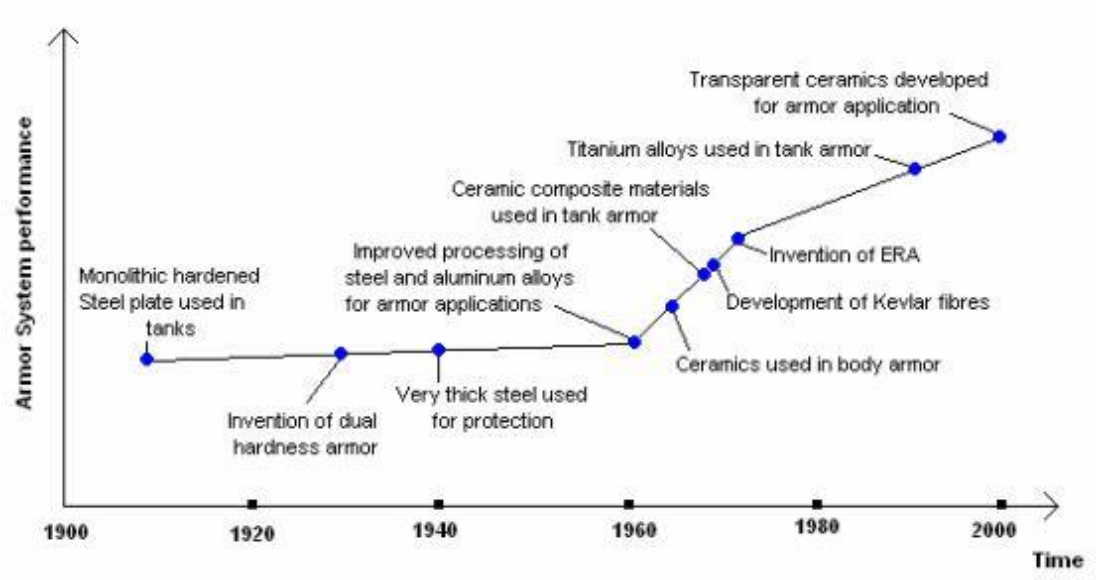

Figure 2.2 Armor system performance development by time (Bhat, 2007)

Armor designs can be classified two parts as passive and reactive. Reactive armor uses kinetic force to counter the ballistic threat. Passive armor uses material properties to dissipate the impact kinetic energy and categorised as disruptors and absorbers. Disruptors function as the first impact layers of armor systems that erode

the projectile into fragments and thus disperse the energy away from the user. In order to succesfully erode the projectile, disruptors are made from materials that have high strength and high hardness compared to the threat. On the other hand, absorbers work by absorbing the kinetic energy through plastic deformation modes.

Ballistic science can be classified four parts:

- Interior ballistic,
- Intermediate ballistic,
- Exterior ballistic,
- Terminal ballistic.

2.2.1 Interior Ballistic

This theory analyzes behaviour of the projectile before leaving from the barrel. The movement of projectile in the barrel can be explained by the effect of gas to the projectile. The bullet is making pressure to the barrel while the movement. That's why friction occurs between the bullet and barrel. The heated gas maket he barrel so harm that any chemical reaction can be occured between them.

Fire starts by the explosion of gas. This explosion causes movement of bullet by increasing pressure. Pressure increases till the movement of bullet. This is maximum pressure point. After that, pressure reduces about %10-30 of the maximum point. As a result, high acceleration is obtained.

2.2.2 Intermediate Ballistic

This theory analyzes behaviour of the projectile for 1-2 milisecond before and after leaving the barrel. It can be said the gate between interior and exterior ballistic.

2.2.3 Exterior Ballistic

This theory analyzes behaviour of the bullet after leaving the barrel. If the inertia acting on bullet, gravity, aerodynamic forces are known, calculation of orbit of the bullet is getting easier.

2.2.4 Terminal Ballistic

This theory analyzes the effect of the bullet on target. This part of ballistic terminology requires technology and more information about mechanical specification of the bullet and the target. That's why the calculation of damage of bullet on target is more difficult than the other ballistic calculation. Figure 3.2 shows parts of ballistic science.

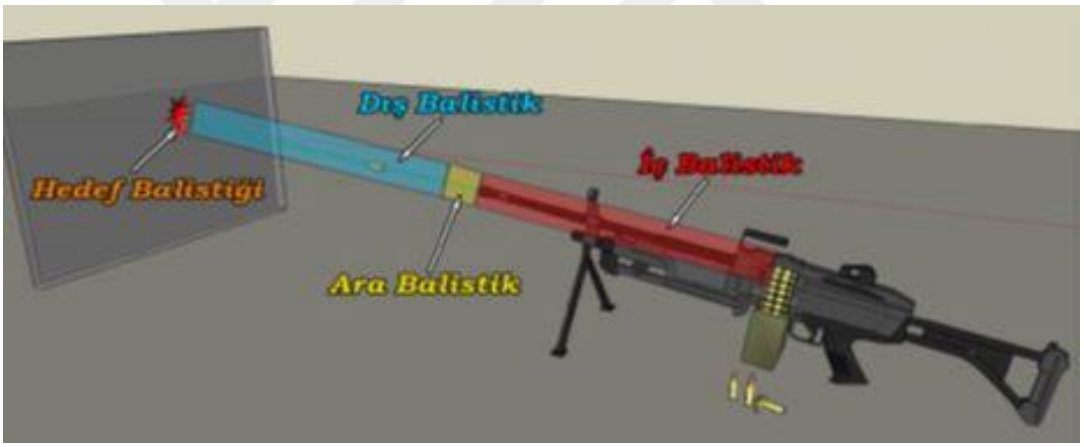

Figure 2.3 Parts of ballistic science (Balistik nedir, n.d.)

CHAPTER THREE
ARMOR MATERIALS

Armor materials are used for civil or military protection at lots of area. Armor materials can be arrayed as steel alloys and composite materials. This materials are changes according to using area. For instance, steel alloys are preferred at military vehicle and composite materials are preferred for protecting clothing. The most impoortant factor of this choice is density.

3.1 Composite Materials

Composite material is a kind of material that manufactured by combining two or more different materials. These materials are used at lots of area because of their different specifications. Urbanizm, housing appliances, electric and electronic industry, aviation industry, automotive industry, construction industry, agriculture and some of application area of composite materials. High structural strength, easy forming, electrical specifications, corrosion and chemical resistance, heat and fire resistance are also some of advantages of composite materials.

On the other hand, composite materials are used for protection clothing.

3.2 Armor Steels

Armor steels are kind of isotropic material like carbon steels or stainless steels. But differences of heat treatment and chemical compound of armor steels make them more strength, tough and hard. That’s why armor steels are used for military or some specific projects for high protecting performances.

3.2.1 Ramor Armor Steels

Ramor armor steels are producted for protection from any explosion and attacking by gun. In addition, Ramor steels have excellent ballistic specification because of

their hardness and good strength. Ramor steels branches off Ramor400, Ramor450, Ramor500, Ramor550. Their numbers show their HBW hardness values. Ramor400 and Ramor450 are produced against pressure that consisted of explosion. On the other hand, Ramor500 and Ramor550 are produced for high velocity impact. Table 3.1 shows mechanical properties and Table 3.2 shows chemical compound of Ramor armor steels.

Table 3.1 Mechanical properties of Ramor400, 450, 500, 550 (Ruukki, n.d.)

Ruuki Ramor	Yield Strength (MPA)	Tensile Strength (MPa)	Elongation %	Hardness (HBW)	Impact Strength (^{o}C)	All Direction Charpy (J)
Ramor400	1100	1300	8	360-450	-40	20
Ramor450	1100	1280	9	420-480	-40	35
Ramor500	1450	1700	7	480-560	-40	20
Ramor550	1550	1850	7	540-600	-40	16

Table 3.2 Chemical compound (%) of Ramor400, 450, 500, 550 (Ramor zırh çeliği, n.d.)

Ruuki Ramor	C	Si	Mn	Cr	Ni	Mo	B
Ramor400	0.24	0.70	1.50	1.00	1.00	0.70	0.005
Ramor450	0.25	0.70	1.50	1.00	2.00	0.70	0.005
Ramor500	0.32	0.70	1.50	1.00	2.00	0.70	0.005
Ramor550	0.36	0.60	1.40	1.50	2.50	0.80	0.005

Some applications of Ramor steels:

- Military vehicles and equipments,
- Shooting ranges,
- Money exchanges counters,
- Security conteiners.

3.2.1.1 Ramor500 Armor Steel

Ramor500 armor steels are producted against high velocity impact. Also it is used at automotive industry to make vehicle more light. For instance, on-board equipment of a concrete mixer can be manufactured by using Ramor500 steel with a thinner plate than structural steel. So it provides more dynamic efficiency and fuel economy.

3.2.1.1.1 Processing Capability of Ramor500. Ramor500 is suitable for general welding methods.

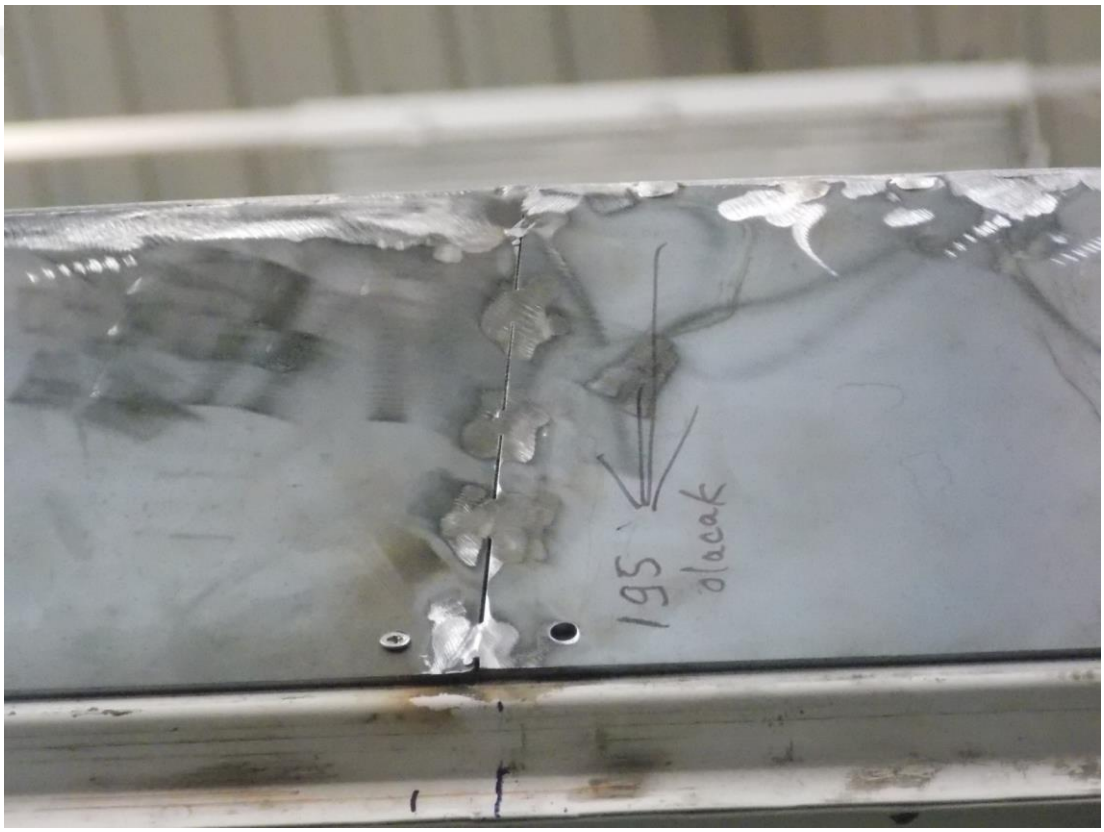

Figure 3.1 MAG welding on Ramor500 armor steel.

Ramor500 is not completely suitable for bending. Bending capacity reduces with the thickness. For example, 3mm plate can be bended maximum about 30^{o}. These value can be change due to the temperature. Figure 3.2 shows the plate that bended 30^{o} for three times to make 90^{o} corner.

Figure 3.1 and Figure 3.2 were published with the permission of Katmerciler Araç Üstü Ekipman A.Ş.

Figure 3.2 Ramor500 plate bended 30^{o} for three times.

On the other hand, bending radius is an important factor for flanging. Minimum bending radius of Ramor armor steels for cold forming are given in Table 3.3 and flanging methods and tools are given in Figure 3.3.

Table 3.3 Minimum bending radius of Ramor steels (Ramor protection steels, n.d.)

Ruuki Ramor	Thickness t<20mm
Ramor400	5 x t
Ramor450	4 x t
Ramor500 and 550	6 x t

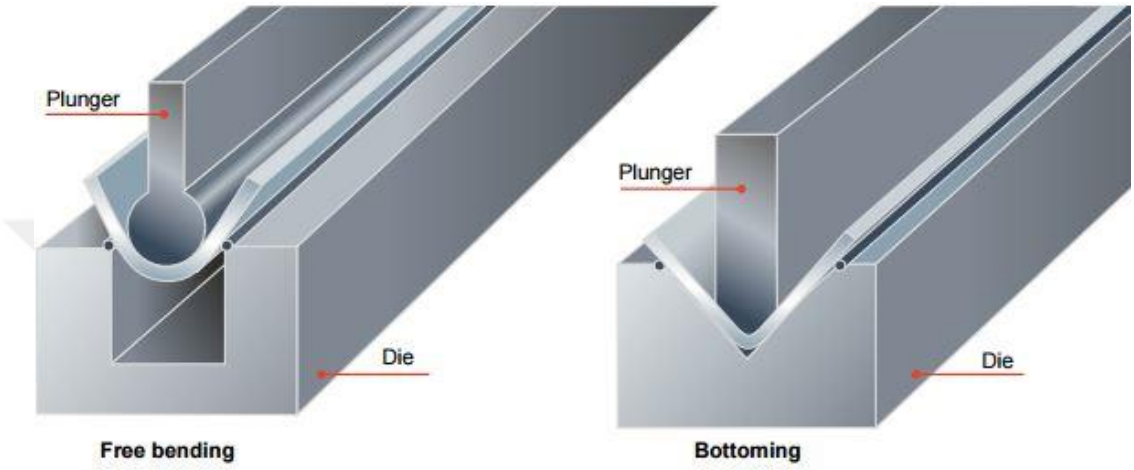

Figure 3.3 Flanging methods of Ramor steels (Flanging, raex wear resistant steels, ultra high strength optim qc steels, n.d.)

Ramor500 is suitable for laser and plasma cutting. But preferred cutting method is water jet because the ballistic properties of cut edge will not lose it's ballistic structure.

If mechanical cutting processes is chosen, some of factors must be watched out. First of all, cutting blades must be sharp enough. If guillotine will be used for cutting, clearance distance and cutting angle must be set carrefuly. For 6mm thick plates, a clearance of 8-10% of plate thickness is sufficient, whereas a 10 mm thick plate requires a 10-15% clearance.

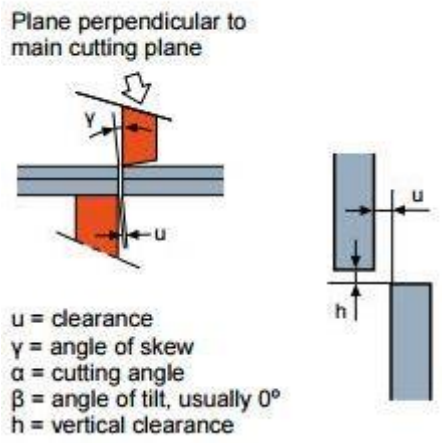

Figure 3.4 Important factors for guillotine shearing (Hot rolled steel sheets, plates and coils mechanical cutting, n.d)

Ramor steels are suitable for machining such as drilling, thread cutting, sawing, milling and turning but workers must pay attention some instructure. First of all the machine must be rigid and stable. The workpiece must be clamped as rigidly. Long tool holders and spindle overhangs must be avoided. Sufficient feed and depth of cut must be used. Cutting fluids must be used during the operation. Cutting speed must be lower in dry cutting. The machining tools must be selected using the manufacturers' data sheet. Table 3.4 shows drilling information for Ramor500.

Table 3.4 Drilling information of Ramor500 (Machining, n.d.)

Machining Tool	**Drill Diamater (mm)**	**Feed Rate (mm/rev)**	**Feed Rate (mm/minute)**	**Cutting Speed (m/minute)**	**Speed of Rotation (rpm)**
Uncoated HSS-Co Drill	5	0.10	20	3	200
	15	0.15	12	4	85
	25	0.20	8	3	40
Hard Metal Bit	16	0.15	120	40	800
Solid cemented Carbide Drill	8.7	0.10	150	40	1500

Maximum recomended heat treatment is +180^{o}C.

3.2.1.1.2 Finding Mechanical Properties of Ramor500. Because of the chemical compound and heat treatment, Ramor500 has high strength properties. This property

is the main reason of high impact strength. On the other hand, Ramor500 is semi-toughness and semi-brittle. While low bending capacity is supporting brittleness, impact responce and explosion resistance are supprting toughness. Table 3.1 shows mechanical properties of Ramor steels.

Mechanical properties are changeable due to temperature. Before tensile testing, the specimen must be stayed at room temperature for 24 hours.

Measurement of specimen is so important for tensile strength. First of all, dimentions of specimen was calculated by using TS EN ISO 6892-1. Figure 3.5 shows lenghts of specimen.

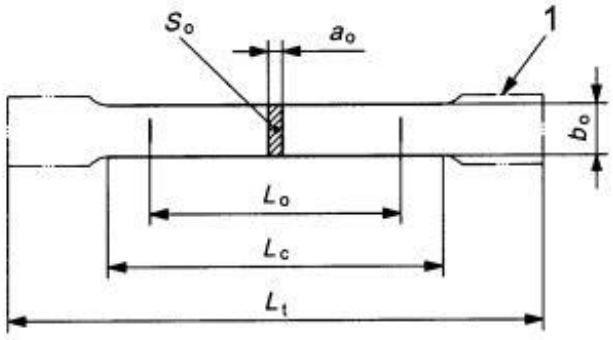

Before tensile testing

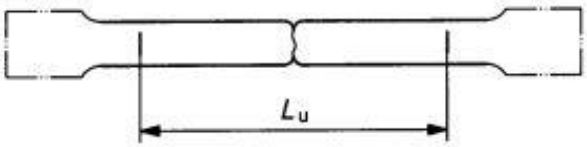

After tensile testing

- a_o: First thickness
- b_o: First width
- L_c: Body length
- L_o: Initial gauge length
- L_t: Total length
- L_u: Final gauge lenth after failure
- S_o: First section area
- 1: Gripping ends

Figure 3.5 Lengths of specimen (TS EN ISO 6892-1, 2011)

According to TS EN ISO 6892-1, ratio between b_o and a_o must be maximum 8mm. Thickness of the specimen is 3 mm. So b_o must be maximum 24 mm and S_o is 72mm^2.

$$L_o = kx\sqrt{S_o} \tag{3.1}$$

k is a constant value and 5.65. so,

$$L_o = 5.65x\sqrt{(3x24)}$$
$$L_o = 47.9\ mm$$

According to L_o, L_c is,

$$L_c = minL_o + \sqrt{S_o} \tag{3.2}$$
$$L_c = 47.9 + \sqrt{72}$$
$$L_c = 56.4\ mm$$

During tensile test, specimens were pulled at constant speed. Using the stroke values obtained, strain values were found by using (3.4) equation. According to variable force and constant first section area (S_o) of the specimen, stress values were found by using (3.5) equation. Finally, stress-strain graph was plotted using obtained datas. Figure 3.6 shows engineering stress-strain graph, Figure 3.7 shows true stress-strain graph of Ramor500 armor steel.

$$\varepsilon = \frac{L - L_o}{L_o} \tag{3.4}$$

Where L_o is first gauge length and L is changeable gauge length.

$$\sigma = \frac{F}{S_o} \tag{3.5}$$

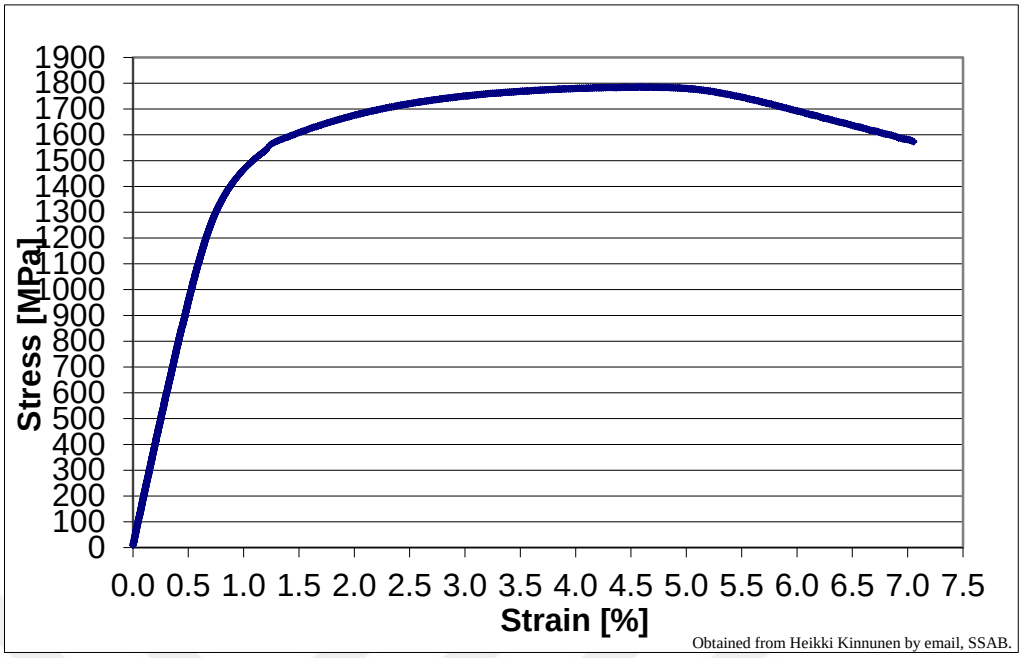

Figure 3.6 Engineering stress-strain graph of Ramor500 armor steel.

According to tensile testing machine, the elastic modulus of Ramor500 is 210 GPa.

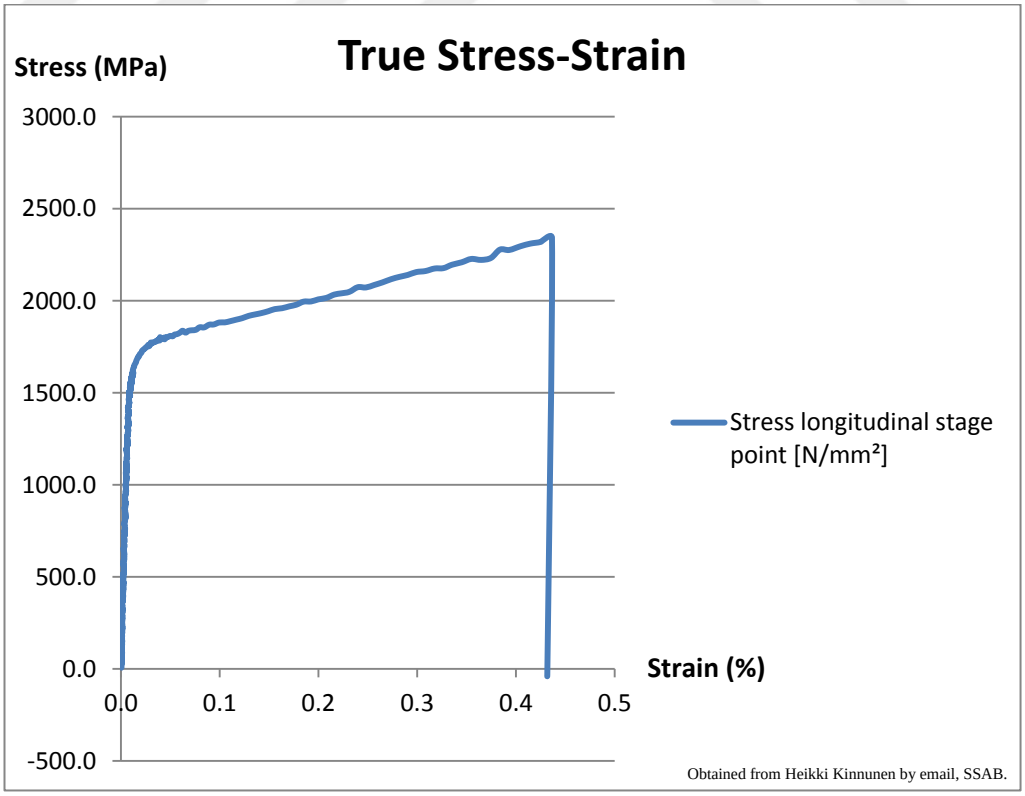

Figure 3.7 True stress-strain graph of Ramor500 armor steel.

CHAPTER FOUR
BALLISTIC STANDARTS

International ballistic testing standarts were developed due to most common used calibers available throughout the military and commercial sectors. The purpose of this standarts is to be establish minimum performance requirements for the ballistic resistance against gunfire. There are 13 different ballistic standarts being used around the World. They are:

- ASTM Ballistic Standarts,
- Australian Ballistic Standarts,
- British Ballistic Standarts,
- Brunswick Ballistic Standarts,
- Canadian Ballistic Standarts,
- European Standarts EN 1063,
- European EN 1522/1523,
- Federal Railroad Administration FRA Ballistic Standarts,
- German DIN Ballistic Standarts,
- MIL-SAMIT Ballistic Standarts,
- National Institute of Justice (NIJ) Ballistic Standarts,
- State Department (SD) Ballistic Standarts,
- Underwaters Laboratory UL 752 Ballistic Standarts.

All designers must use their national standarts to design military vehicles, bulletproof vest, etc.

On the other hand, body armor manufacturers must use these standarts, too.

4.1 National Institute of Justice (NIJ) Ballistic Standarts

This standart is classified into six types by level of ballistic performance. These are:

- NIJ LEVEL I,
- NIJ LEVEL IIA,
- NIJ LEVEL II,
- NIJ LEVEL IIIA,
- NIJ LEVEL III,
- NIJ LEVEL IV.

4.1.1 NIJ LEVEL I

This armor protects against .22 LR HV bullets at velocity between 308-332 m/s or .38 Special impacting at velocity between 244-274 m/s.

4.1.2 NIJ LEVEL IIA

This armor protects against 9 mm full metal jacketed round nose (FMJ RN) bullets with nominal masses of 8.0 g impacting at a minimum velocity of 332 m/s or less and .40 S&B caliber full metal jacketed (FMJ) bullets with nominal masses of 11.7 g impacting at a minimum velovity of 312 m/s or less. Level IIA body armor is well suited for full-time use by police departments, particularly those seeking protection for their officers from lower velocity .40 S&B and 9 mm ammunition.

4.1.3 NIJ LEVEL II

This armor protects against .357 Magnum jacketed soft-point bullets with nominal masses of 10.2 g impacting at velocity of 425 m/s or less and against 9 mm full-jacketed bullets with nominal velocities of 358 m/s. It is also protects against Level IIA threats. Level II body armor is heavier and more bulky than Level IIA. It is worn

full time by officers seeking protection against higher velocity .357 Magnum and 9 mm ammunition.

4.1.4 NIJ LEVEL IIIA

This armor protects against .44 Magnum, Semi Jacketed Hollow Point (SJHP) bullets with nominal masses of 15.55 g impacting at velocity of 426 m/s or less and against 9 mm full-metal jacketed bullets with nominal masses of 8.0 g impacting at velocity of 426 m/s or less. It also provides protection against most handgun threats as well as the Level IIA and II threats. Level IIIA body armor provides the highest level of protection currently available from concealable body armor and is generally suitable for routine wear in many situations. However, department located in hot, humid climates may need to evaluate the use of Level IIIA armor carefully.

4.1.5 NIJ LEVEL III

This armor, normally of hard or semirigid construction, protects against 7.62 full-metal jacketed bullets with nominal masses of 9.7 g impacting at velocity of 838 m/s or less. It also provides protection against threats such as 223 Remington, 30 Carbine FMJ, and 12 gauge rifled slug, as well as Level IIA through IIIA threats. Level III body armor is clearly intented only for tactical situations when the threat warrants such protection, such as barricade confrontations involving sporting rifles.

4.1.6 NIJ LEVEL IV

This armor protects against .30-06 caliber armor-piercing bullets with nominal masses of 10.8 g impacting at velocity of 868 m/s or less. It also provides at least single-hit protection against the Level IIA through III threats.

Level IV body armor provides the highest level of protection currently available. Because this armor is intented to resist “armor piercing” bullets, it often uses ceramic metarials. Such materials are brittle in nature and may provide only single-shot

protection since the ceramic tends to break up when struck. As with Level III armor, Level IV armor is clearly intended only for tactical situations when the threats warrants such protection.

Table 4.1 National Institude of Justice (NIJ) ballistic standarts (NIJ, 2008)

Standart	**Bullet**	**Bullet Weight (g)**	**Distance (m)**	**Striking Velocity (m/s)**	**Number of Shots**	**Sample Size**
NIJ LEVEL IIA	9 mm Luger FMJ RN	8	5	332	5	300x300
NIJ LEVEL II	.357 Magnum JSP	10.2	5	425	5	300x300
NIJ LEVEL IIIA	9mm FMJ or .44 Magnum JHP	15.6	5	426	5	300x300
NIJ LEVEL III	7.62 mm NATO FMJ	9.6	5	838	5	300x300
NIJ LEVEL IV	30.06 M2 AP	10.8	5	868	1	300x300

After shooting to the specimen, three possibilities can be occured. The first is skipping or deformation of bullet. It means ballistic test is successful. The second is bullet makes a hole on the specimen but can not pass through the specimen (Penetration). The last one is perforation. That means bullet makes a hole on the specimen and goes its own way.

Depending on Table 4.1, two different ways are available for passing the ballistic test. First of all, we can stick paste behind the specimen. After shooting to the specimen, displacement on the paste must be under 44 mm. If not, the material is not suitable for usage. So, that mean, the specimen does not pass the test.

On the other hand, second way to check the test result is lighting. After shooting to the specimen, we must set light from back of the specimen. If lighting could be

seen front of the specimen, the material is not suitable for usage. So, the specimen does not pass the test. Figure 4.1 shows a part of armor glass after the ballistic test of BR6. Although displacement under 44 mm, huge cracks and holes were occured behind the glass. It means this glass is not usage for any protection.

Figure 4.1 Test result of armor glass according to BR6.

Figure 4.1 Test result of armor glass according to BR6 (continue).

CHAPTER FIVE
BULLETS AND EXPERIMENT OF NIJ LEVEL IIIA

5.1 Parts of Bullets

Bullet is a piercing and explosive stuff and used for protection or attacking. Bullets have three parts. First one is core. This part is fired and makes damage on targets. Second is gunpowder. When gunpowder fired, bullet is flinged from the barrel because of high pressure. The last part is Shell. This part is a kind of cylinder and contain gunpowder inside.

There is an igniter behind the Shell and allows firing the gunpowder when the trigger was pushed. Figure 5.1 shows parts of a bullet.

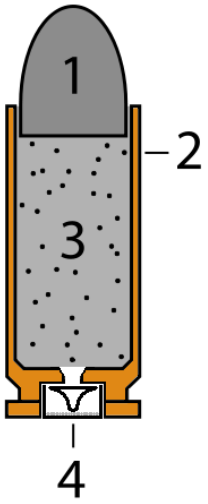

Figure 5.1 Parts of a bullet (Bullet, n.d.)

According to figure,

1. Lead core,
2. Shell,
3. Gunpowder,
4. Igniter.

5.2 9mm FMJ (Full Metal Jacket) Bullets

These bullets are consisting of lead core and copper plated jacket. Copper plated jacket just covers lead core except rear side. Copper plate is more strength than lead core, that's why while tipped bullets are for use against soft targets only, whereas full metal jacketed bullets can be used effectively against both soft and hard targets. In addition, FMJ bullets have less expand capacity than tipped bullets. Figure 5.2 shows compression test of copper jacket of 9 mm FMJ. According to results of compression test, Young's modulus of copper is 42.5 GPa and higher than lead (16 GPa). During the compression, we can see two buckling modes of copper jacket.

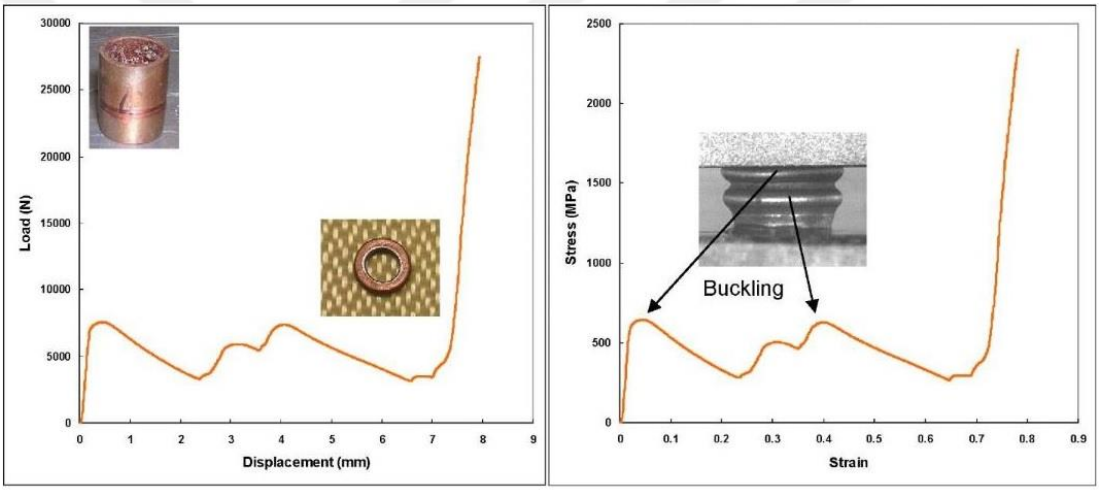

Figure 5.2 Compression test of copper plated jacket (Proulx, 2011)

5.3 .44 Remington Magnum

The .44 Remington Magnum, or simply, .44 Magnum (10.9x33 mmR) designed for revolvers. This bullets are large and heavy bullet with high velocity for a handgun. In its full powered form, it produces so much recoil and muzzle blast that it is generally considered to be unsuitable for use as a police weapon. This weapons have more impact energy when fired from the same weapon. Figure 5.3 shows .44 Magnum bullet.

Figure 5.3 .44 Remington Magnum bullet.

5.4 Ballistic Test Contrivance

For ballistic test of Ramor500 armor steel we must follow instructions in Table 4.1. According to NIJ LEVEL IIIA, the specimen in 300x300x3 mm must be placed 5 m away from the barrel and must be shot for 3 times with 9 mm full metal jacket (FMJ) bullet. There must minimum 120 mm between shooting points because not to effect each other by shock wave. In addition, there must minimum 70 mm between shooting points and holding jaws. The bottom of target must 1m above from the ground. Minimum 2 speedometer must be placed between the barrel and target. So, impact velocity can be calculated by knowing speed reduction between two speedometer. Figure 5.4 shows a representative ballistic test contrivance. But, in the the test, we will shoot to Ramor500 armor steel in 500x500x3 mm from 5 m away from the barrel for 3 times and discuss the results. Figure 5.5 shows real ballistic test contrivance.

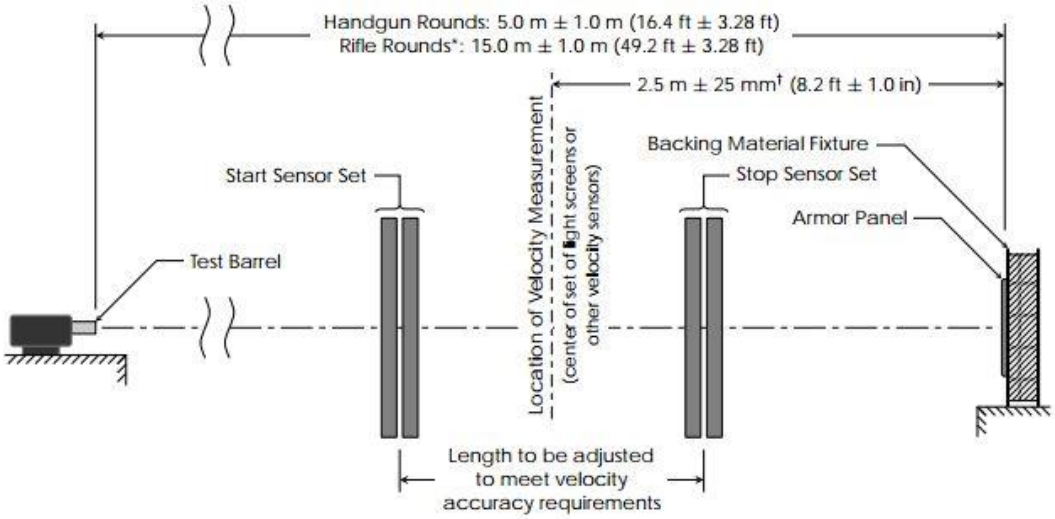

Figure 5.4 Representative ballistic test contrivance (Bhat,2007)

Figure 5.5 Real ballistic test contrivance.

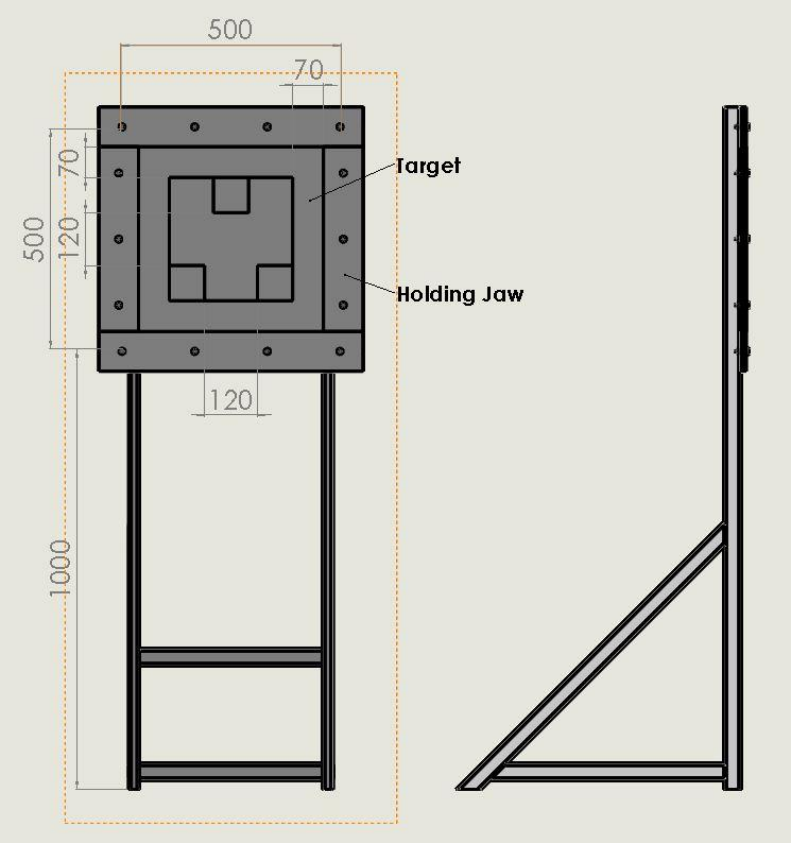

Figure 5.5 Real ballistic test contrivance (continue).

5.5 Ballistic Test Processing

Before shooting test, we must take care of some precautions. Security is the most importing thing of these precautions. Shooting process must be done away from settlement or at polygons. If shooting process will be done out of polygon, we must get permission from gendarme.

Headphone is necessary during shooting for not to hurt ears because of high noise. In addition, glasses is also necessary for preventing our eyes from hopped particles.

One of the most important thing is, during test processing, there must be nobody nearby the shooting area for not to hurt because of hopping particles of bullet.

The gun must be used by trained personel for minimize the probability of accident.

On the other hand, angle between the bullet and target must be perpendicular. So kinetic energy of the bullet can be transferred completely to the target. If not, parallel component of velocity of bullet causes hopping of the bullet. So it may cause accidents and hurt people. Figure 5.6 shows schematic representation of angle of incidence. Figure 5.7 shows before and after shooting test.

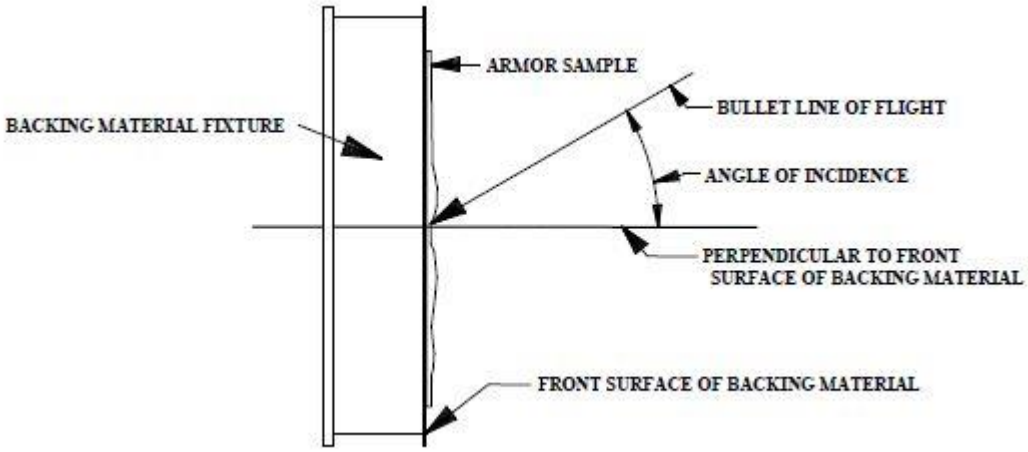

Figure 5.6 Angle of incidence (NIJ, 2008)

Figure 5.7 Before and after shooting.

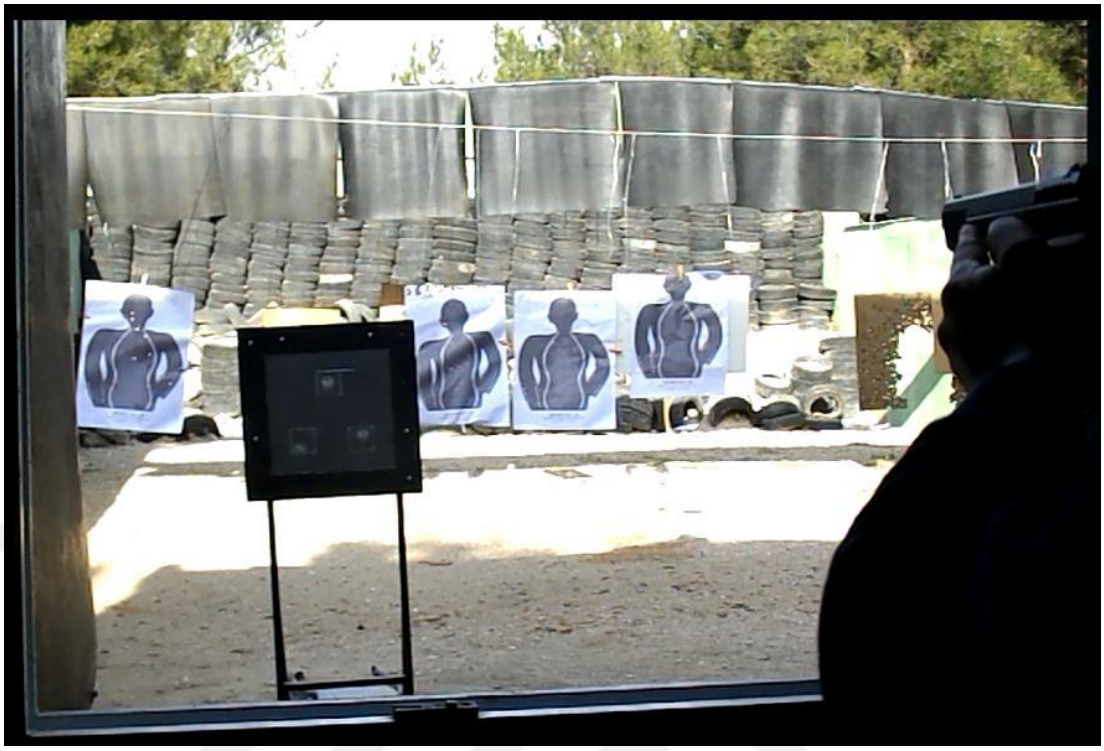

Figure 5.7 Before and after shooting (continue).

Shooting points had must been in squares and police officer succeed the mission perfectly.

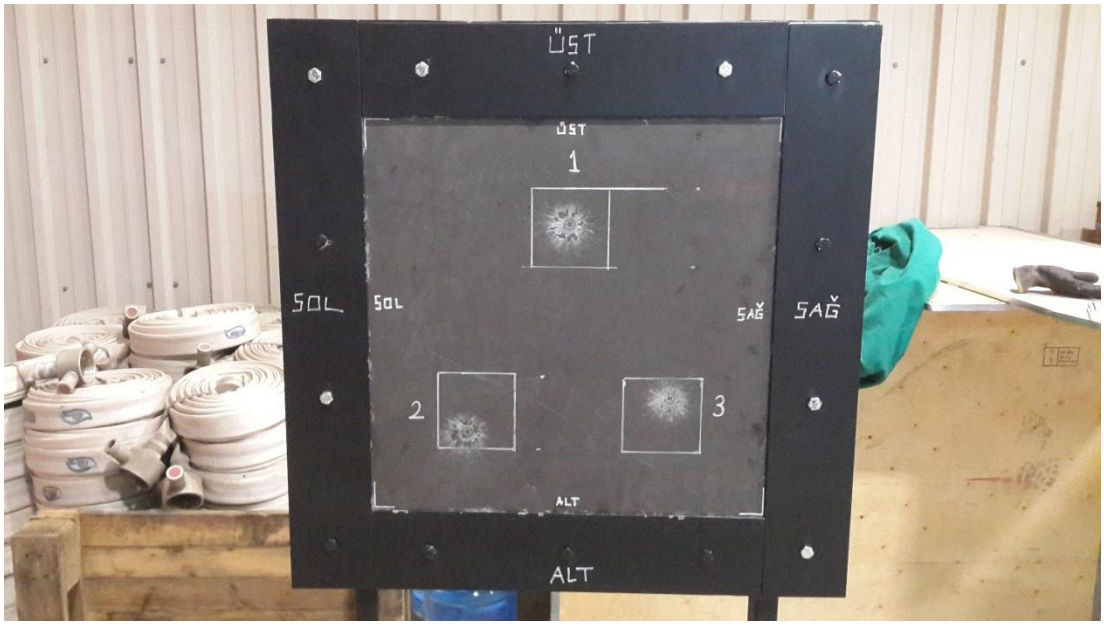

Figure 5.8 Shooting points.

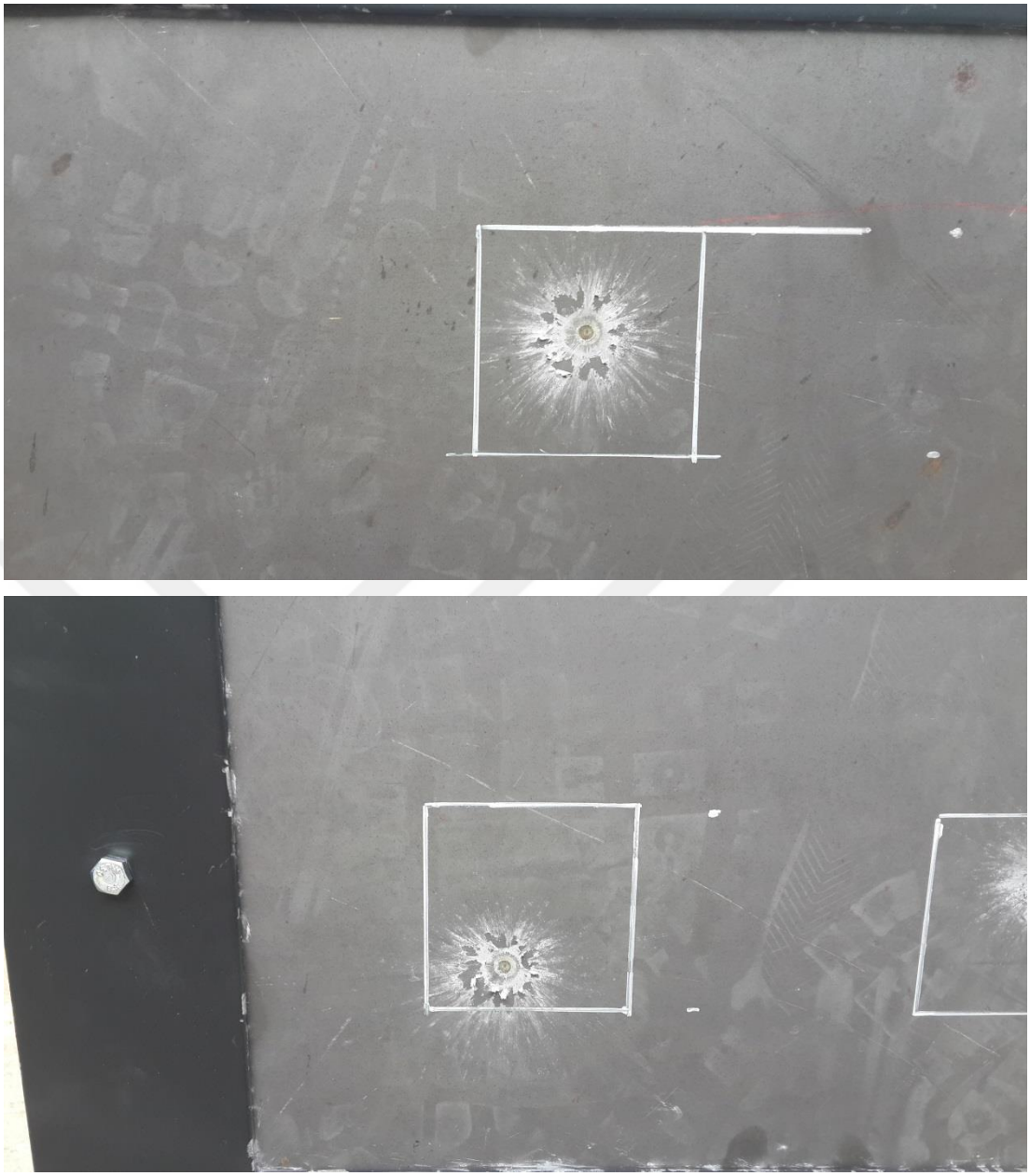

Figure 5.8 Shooting points (continue).

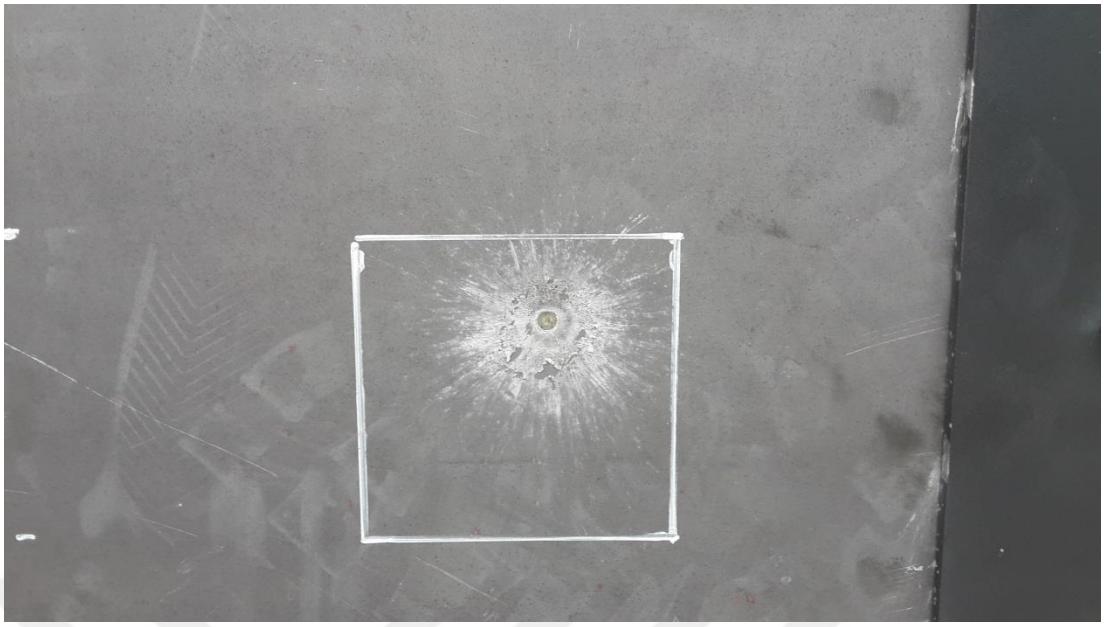

Figure 5.8 Shooting points (continue).

All bullets deformed during the test and no hole or crack was occured on the target. Deformation is too small at the back of the target. No light was seen at the front of the target. It means, Ramor500 armor steel in 3 mm thickness is useful for NIJ LEVEL IIIA.

Since the bullet can not pierce the target, kinetic energy was used to deforme bullet and produce high temperature on contact zone.

After shooting test, when we opened holding jaws, some deformed particles belong to bullet were found between the target and holding jaws. So, this is the proof of high pressure during impact. On the other hand, in Figure 5.8, there are spreaded and sticked stains around shot point. Actually, these stains are also particles of bullet and sticked because of high pressure during impact. Figure 5.9 shows sticked particles between target and holding jaws. Figure 5.10 shows deformed bullet after testing.

Figure 5.9 Sticked particles between the target and holding jaws.

Figure 5.9 Sticked particles between the target and holding jaws (continue).

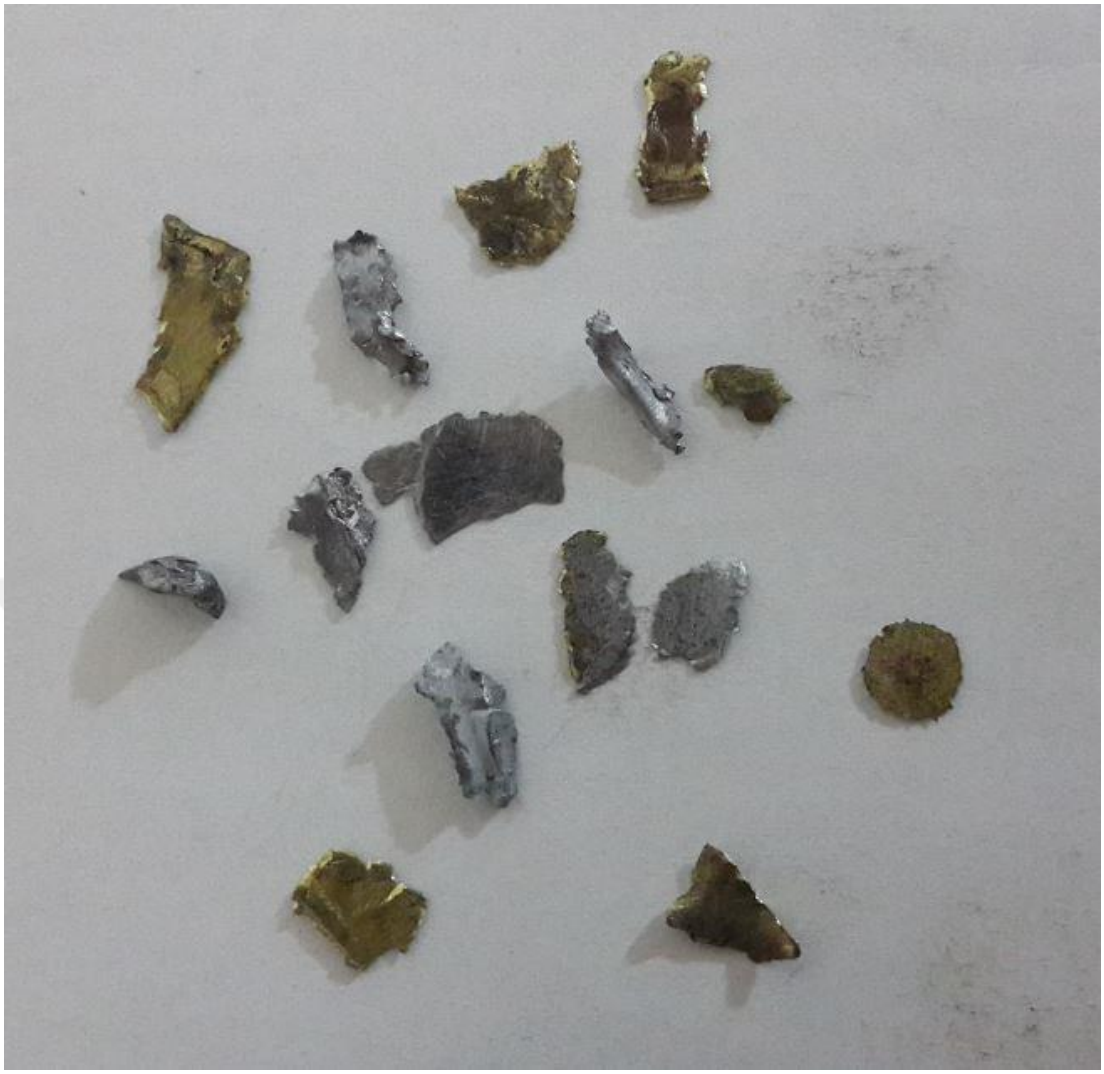

Figure 5.10 Deformed bullet after ballistic test.

After simulation of ballistic perforation, the shape of bullet is expected as the shape in Figure 5.10.

CHAPTER SIX
BALLISTIC SIMULATION

6.1 Theory Overview

Structural impact involves events such as plastic flow at high strain rates, possible local increase of temperature and material fracture. To describe the various phenomena taking place during ballistic penetration, it is necessary to characterize the behaviour of materials under impact-generated high strain rate loading conditions. This characterization involves not only the stress-strain responce at large strains, different strain rates and temperatures, but also the accumulation of damage and the mode of failure. Such complex material behavior involving fracture is difficult to describe in analytical models. Accordingly, different mathematical models are needed to describe plastic flow and fracture, Johnson-Cook is one of them. Johnson-Cook model is a coupled material model capturing viscoplasticity (rate dependent plasticity) and ductile damage, deveoped for impact and penetration problems.

Johnson-Cook plasticity model have been created by Gordon R. Johnson and William H. Cook in 1983. It is suitable for high strain rate deformation of many materials including most metals. Moreover, it is generally used in adiabatic transient dynamic analyzes.

In Johnson-Cook plasticity model equivalent stress is assumed to be of the form:

$$\sigma_{eq.} = (A + B.(\mathrm{E}^{p})^{n}).\left[1 + C.\log\left(\frac{\dot{\mathrm{E}}^{p}}{\dot{\varepsilon}_{o}}\right)\right].\left(1 - \hat{T}^{m}\right) \qquad (6.1)$$

Where,

$$\hat{T}=0, \quad for \quad T < T_{r},$$

$$\hat{T} = \frac{T - T_r}{T_m - T_r}, \quad for \quad T_r \leq T \leq T_m \tag{6.2}$$

$$\hat{T} = 1 \quad for \quad T > T_m$$

In equation (6.1) ε^p is the equivalent plastic strain, A is the yield stress, B is the hardening constant, n is the hardening exponent, m is the thermal softening exponent. C and $\dot{\varepsilon}_o$ are required to define Johnson-Cook rate dependence.

In equation (6.2) $\hat{T}$ is a dimentionless temperature, T is the current temperature, T_m is the melting temperature and T_r is the referance temperature.

In equation (6.1), Johnson-Cook eq. consists of three brackets. The first one is the influence of plastic strain, the second is the influence of strain rate and the last bracket is the influence of temperature change.

If impact responce is wanted to solve, these parameters (A, B, n, C, m) must be obtained by experimental processes. For all of these, the true stress-strain curve must be plotted firstly.

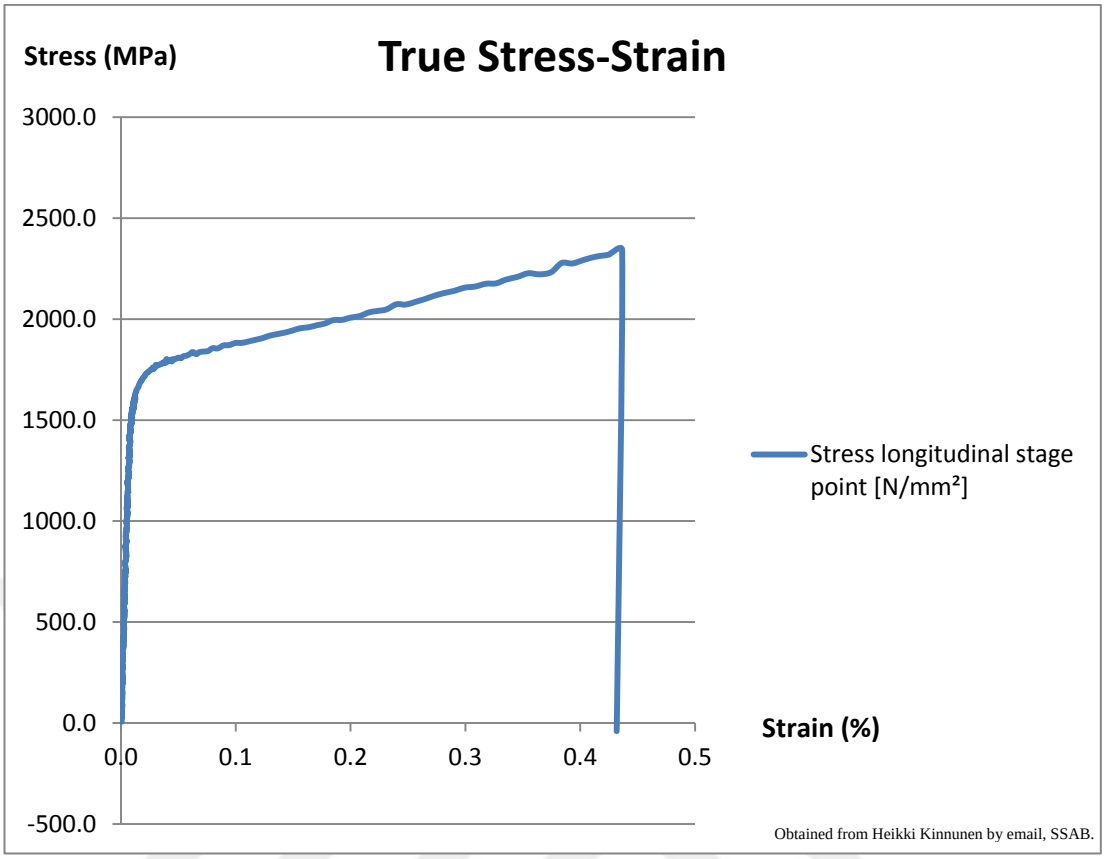

Figure 6.1 True stress-strain curve.

The plastic zone of this curve is representing the first bracket of J-C equation and this stress-strain values are fitted with $\left(A + B.\varepsilon_p^n\right)$ by using MATLAB (Figure 6.2).

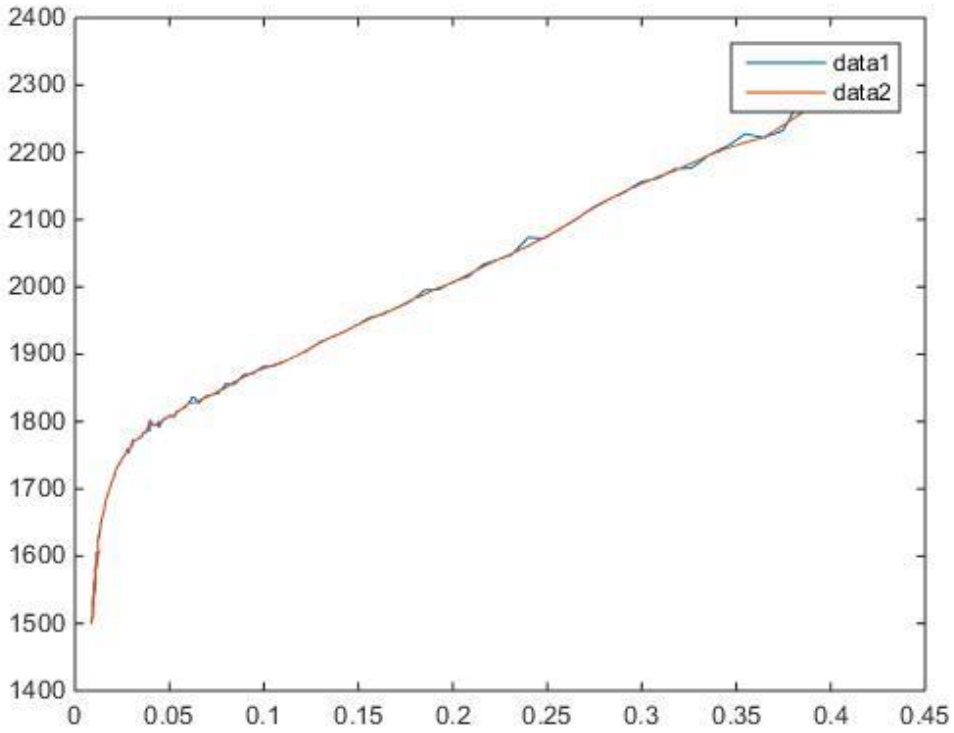

Figure 6.2 The plastic zone of true stress-strain curve.

In this graph, plastic zone was plotted between 1450 -2300 MPa, approximately. In addition, data 1 represents the curve of plastic stress-strain curve. Data 2 represents the smoothed version of data 1. After the fitting of $\left(A + B.\varepsilon_p^n\right)$ with the plastic curve, we obtained that A is 1450 MPa, B is 1288 MPa and n is 0.483. We know that A is the yield stress and B is the hardening modulus. n value must be $0 \leq n \leq 1$ normally, and represents the value of hardness of materials (Figure 6.3).

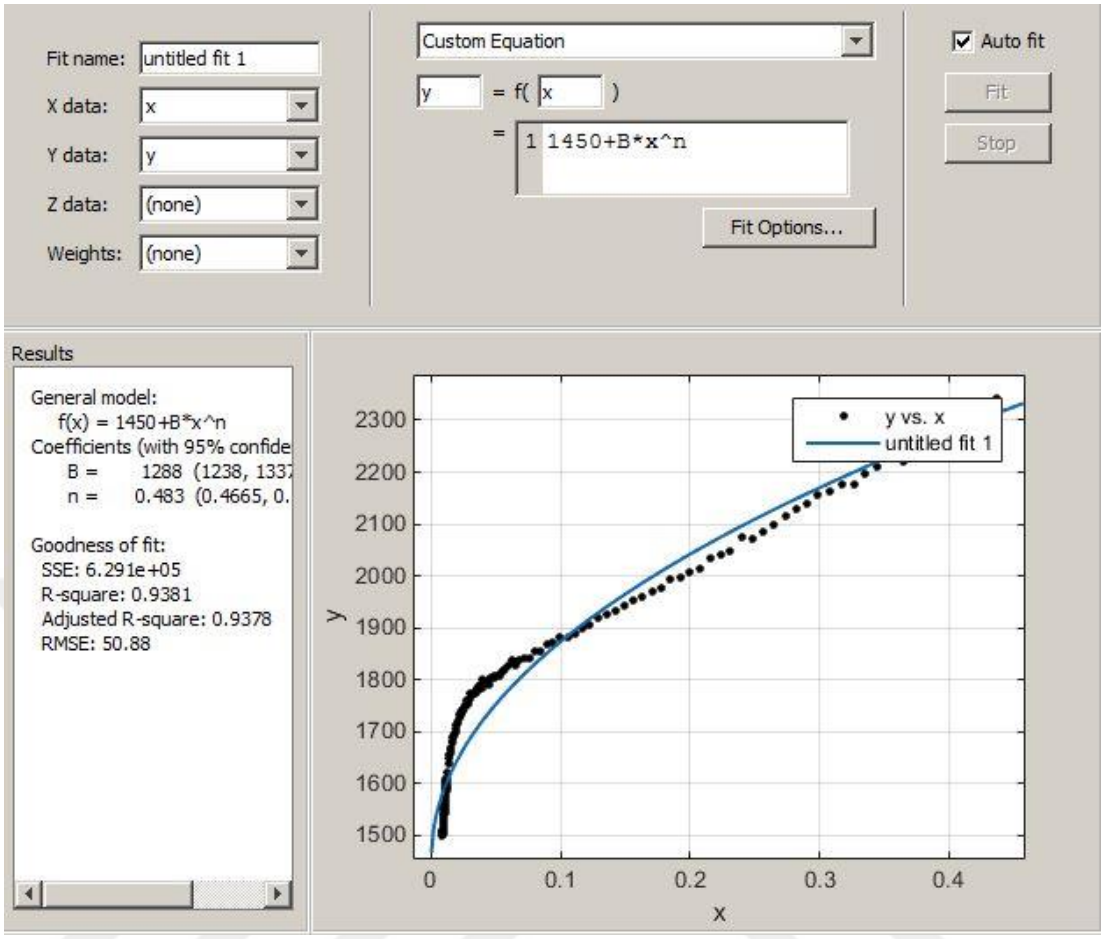

Figure 6.3 A, B and n values.

On the other hand, the second bracket is the influence of strain rate and fitted with $1 + C.\ln\left(\frac{\dot{\varepsilon}}{\dot{\varepsilon}_o}\right)$, where $\dot{\varepsilon}$ is strain rate and $\dot{\varepsilon}_o$ is the referance strain rate. To obtain C, Hopkinson Split Bar test must be done. Figure 6.4 shows SHPB of Ramor500 at different strain rates; 500, 1400 and 2500 s^{-1}, respectively.

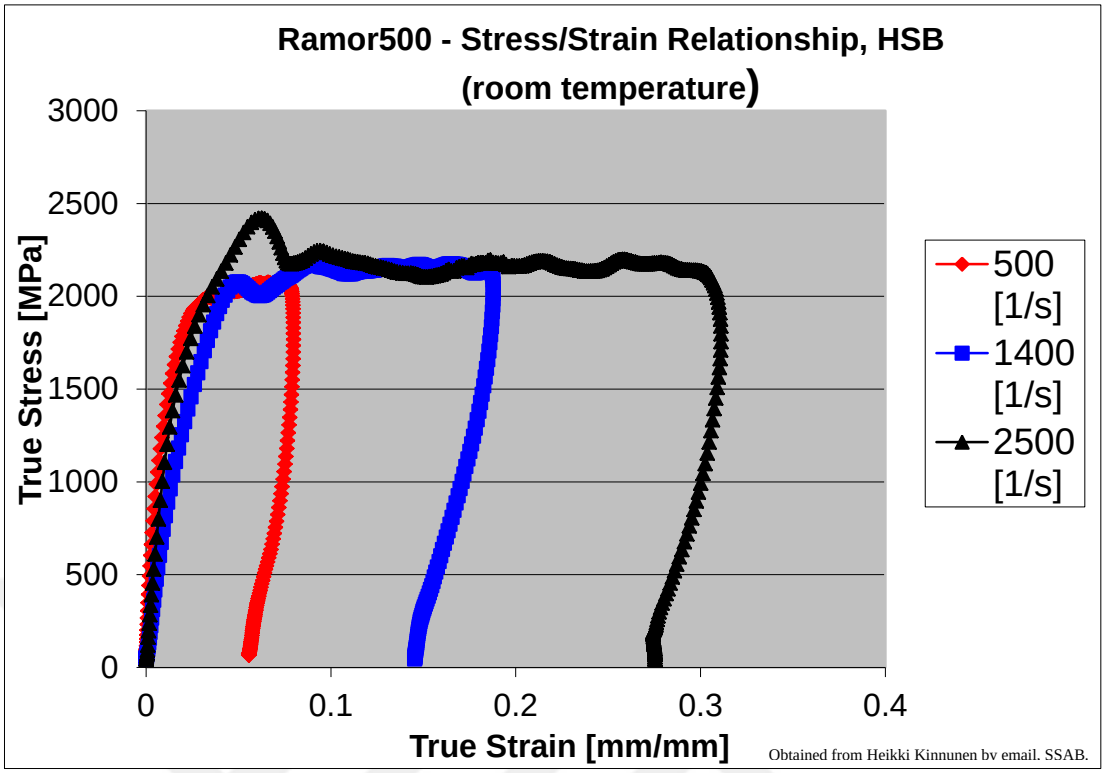

Figure 6.4 SHPB test of Ramor500.

Figure 6.5 shows yield stresses correspond to strain rates. To find C, we must fit this curve with $1 + C.\ln\left(\frac{\dot{\varepsilon}}{\dot{\varepsilon}_o}\right)$ on MATLAB. After the fitting, we obtain C, which is 0.02131 (Figure 6.6)

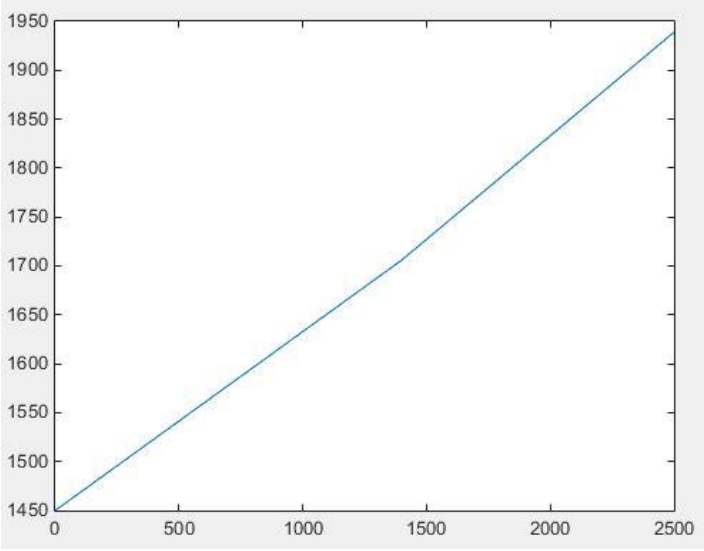

Figure 6.5 Stress-Strain rates curve.

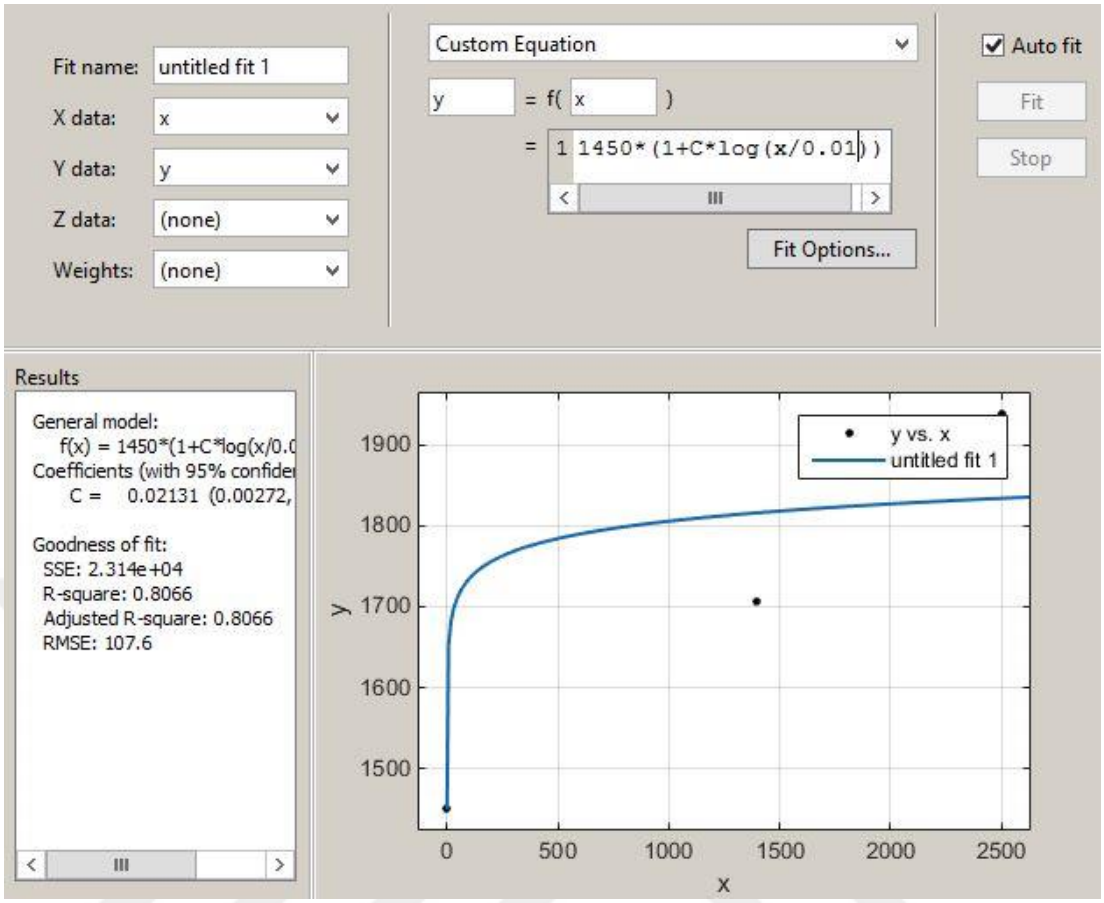

Figure 6.6 Strain rate constant.

Finally, the third bracket is the influence of temperature and fitted with $(1 - \hat{T}^m)$, where $\hat{T}$ is a dimentionless value and equal to $\frac{T-T_r}{T_m-T_r}$ (page 36), m is the temperature softening exponent. To obtain m, we must know yield stresses of the specimen at different temperatures. Thats's why two tensile tests has been done. First one was at 20 ^{o}C and yield stress is 1450 MPa, second one was at 200 ^{o}C and yield stress is 900 MPa. So $\hat{T}$ is 0 and 0.116279, respectively.

After fitting of $(1 - \hat{T}^m)$ with the curve, we obtain m is 0.4505 (Figure 6.7)

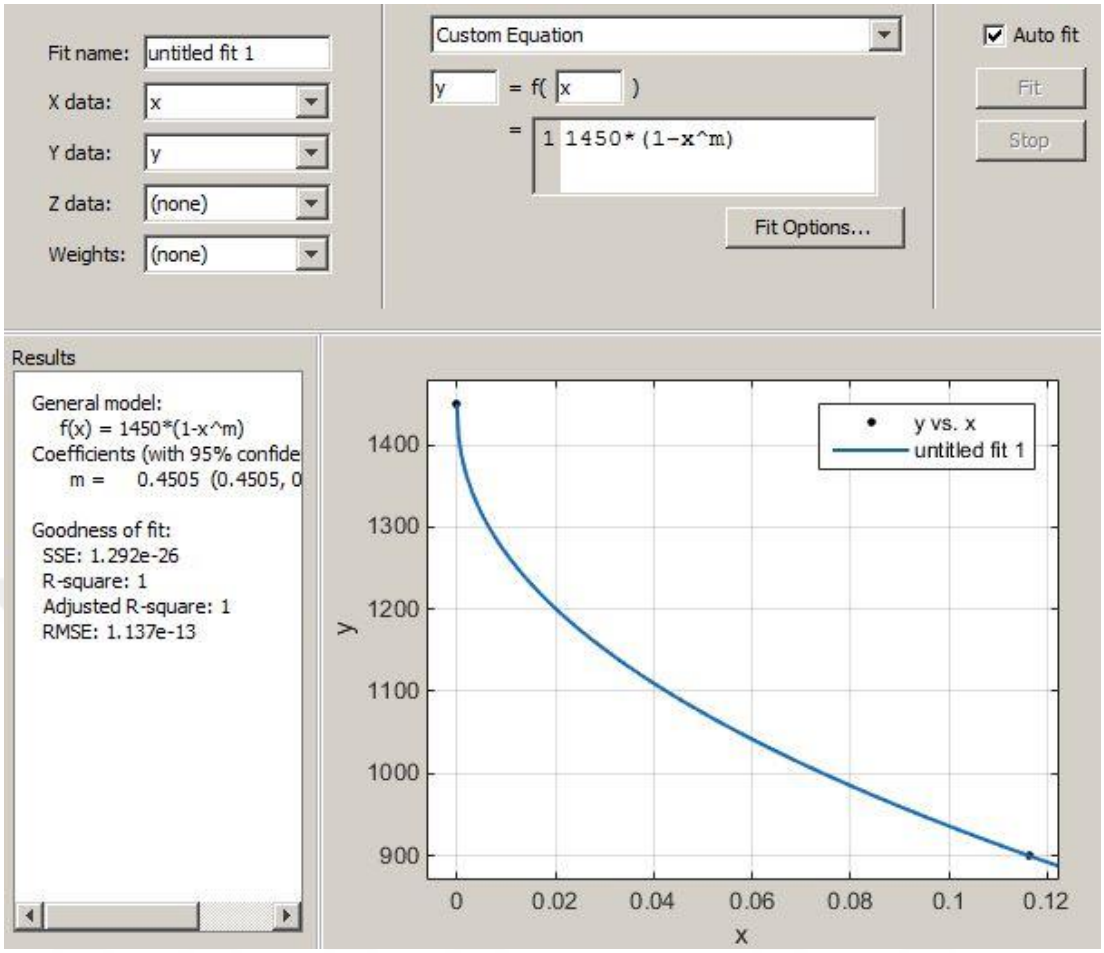

Figure 6.7 Thermal softening exponent.

6.2 Background of Numerical Simulation

Simulation of the ballistic perforation is a complex process. In addition, it is needed to find a material which is suitable, resistant of high stress, high pressure and cracks.

In a shooting test, the structural responce of the material can vary. When a material is stressed by ballistic loading, shock waves are capable of creating pressure of a magnitude that can significantly exceed the material's strength. At the early stages of the event, a solid material can be considered as a compressible fluid. After a while, strength effects appear again (Abaqus Technology Brief, 2012).

For NIJ LEVEL IIIA, 9 mm FMJ projectile was used for shooting. Young's modulus and yield strength of projectile are 16 GPa and 10.3 MPa, respectively.

As target, Ramor500 armor steel in 500x500x3 mm dimentions were used. Young's modulus and yield strength of Ramor500 are 210 GPa and 1450 MPa, respectively.

6.3 Analysis Approach

For ballistic test, constitutive model was created by using Solidworks and transferred to Explicit Dynamic modulus in Ansys. In any impact simulation, the accuracy of results depend on three matters:

- Meshing,
- Constitutive model,
- Material datas.

6.3.1 Explicit Dynamic Modulus

Explicit Dynamic is a kind of simulation method of dynamic loading. Impact response, short-duration high-pressured loadings can be solved easily by using Explicit Dynamic. Because of the high prize or impossibilities of experimental solution of these specialized problems, packet simulation programs are needed.

Explicit Dynamic show us easily how to response these constructions are in severe loading or situations such as;

- Impact or penetrations,
- Drop tests,
- Blast effects,
- Crash of vehicles,
- Shock wave propagations,

- Non-linear material behaviour,
- Fragmentation,

and any cases cause large deformations and strains.

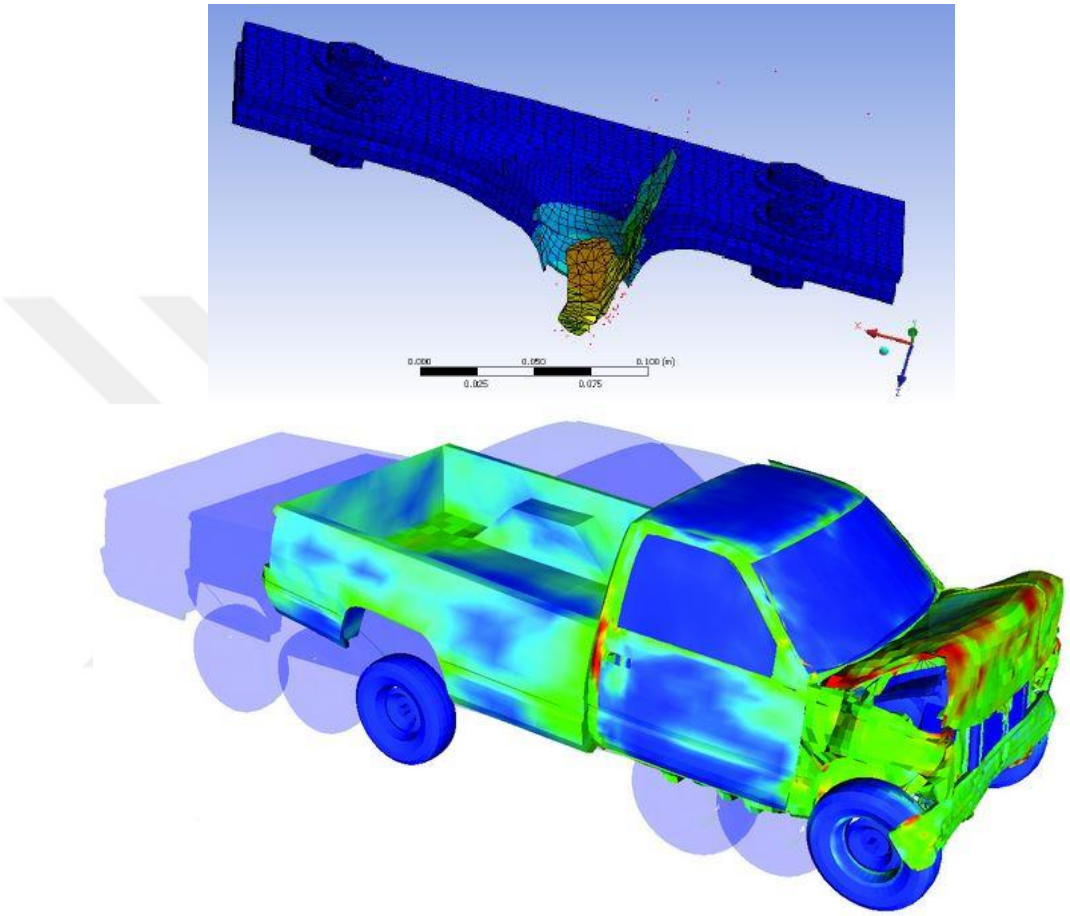

Figure 6.8 Sample applications-Explicit Dynamic (Engineering, n.d.)

The formulation of Explicit Dynamic based on;

$$M.\ddot{X} + C.\dot{X} + K.X = F \tag{6.3}$$

Where,

M : Mass,

C : Damping,

K : Stiffness,

X : Nodal displacment,

F : Externally applied nodal force.

The approach used in Explicit Dynamic based on the calculation of unknown displacements, velocities and accelerations at the current time.

If the time step size (Δt) is set and all primary solution variables are known up to time t, then the calculation of solution can be accomplished at time t+Δt. In fact, the results at time t is the initial condition of the second step at time t+Δt. The integration goes in this wise up to the final step.

$$\dot{X} = \frac{1}{\Delta t}\left(X_{(t+1)} - X_t\right) \tag{6.4}$$

$$\ddot{X} = \frac{1}{2\Delta t}\left(\dot{X}_{(t+1)} - \dot{X}_t\right) \tag{6.5}$$

In equation (6.4), X_t is displacement of per nodes at time t, $X_{(t+1)}$ is displacement of per nodes at time t+1. So, the derivation of substruction of displacements gives the velocity of per nodes.

In equation (6.5), $\dot{X}_t$ is velocity of per nodes at time t, $\dot{X}_{(t+1)}$ is velocity of per nodes at time t+1. So, the derivation of substruction of velocities gives the acceleration of per nodes.

In dynamic simulations, four kind of solver methods are used. These are:

- Lagrange,
- Euler,
- Arbitrary Lagrangian-Eulerian (ALE),
- Smoothed Particle Hydrodynamics (SPH).

Explicit Dynamic use Lagrange method among these methods.

6.3.2 Meshing

Meshing is one of the critical point in engineering simulations. Reducing meshing size causes increment of total element number and simulation takes more time. On the other hand, increasing meshing size causes unreliable resuts. That's why meshing size must be optimal in simulations.

In addition, meshing type is also important for results of simulation. Different kinds of meshing method can be chosen for different surface modelling.

On the other hand, four kinds of solver method, as we mentioned, use different meshing type (Figure 6.9).

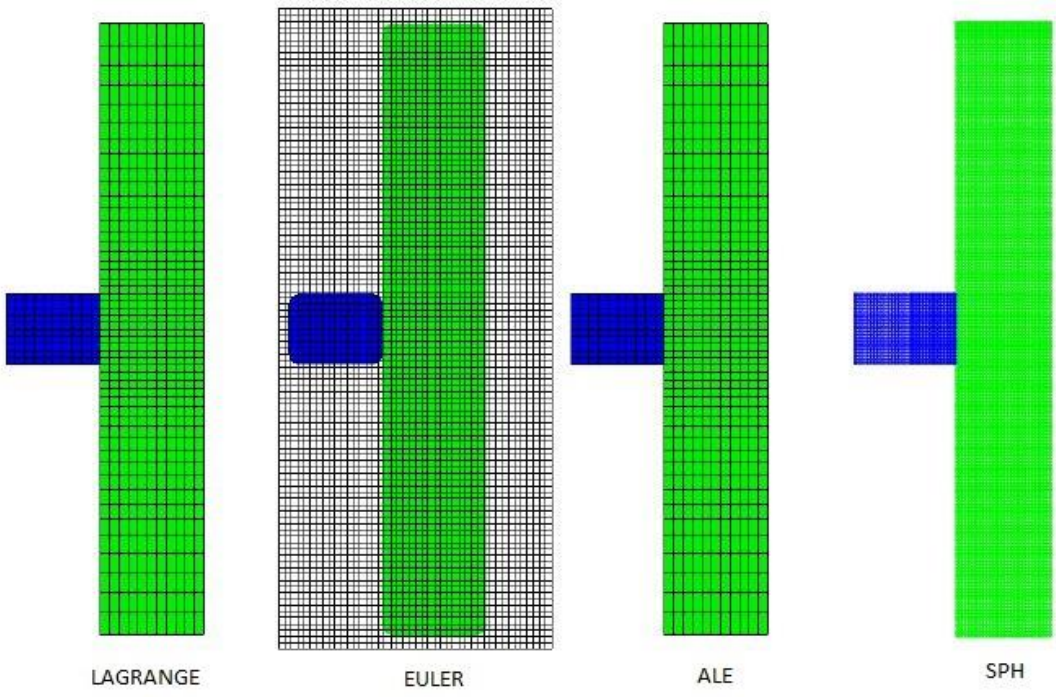

Figure 6.9 Meshing types of solver methods (Quan, Birnbaum, Cowler, & Gerber, 2003)

6.3.3 Constitutive Modelling

Constitutive modelling is an important factor in engineering simulations. If we do not know which way or formulation we must use, the results will not be reliable.

As we mentioned, impact modelling responses as a fluid and metal, respectively. In addition we know that large deformations and strains will be obtained after impact simulation. That's why, Johnson-Cook modelling is the best for this analysis.

6.3.4 Material Datas

Material datas are the heart of any simulations. As we know, responces of materials changing depend on their material datas. Reliable numerical results depend on defining material datas correctly.

6.4 Simulation Process

Simulation process is the part of analysis that we obtain the final results. The truth of this results depend on the truth of input datas and boundary conditions.

At the first stage of this study we will analyze the impact response of Ramor500 plate at different thicknesses against 9 mm FMJ bullet at 430 m/s constant speed and find out the critical puncture thickness of Ramor500 plate.

At the second stage of the study we will try to find out the critical puncture velocity of the bullet on the plate in 3 mm thickness.

Before the beginning of analyze, we must describe materials we will use. Figure 6.10 shows the necessary parameters of Ramor500 and lead.

Properties of Outline Row 3: LEAD

	A	B	
1	Property	Value	
2	Density	11340	kg m^-3
3	Specific Heat	124	J kg^-1 C^-1
4	Johnson Cook Strength		
5	Strain Rate Correction	First-Order	
6	Initial Yield Stress	10,3	MPa
7	Hardening Constant	41,3	MPa
8	Hardening Exponent	0,21	
9	Strain Rate Constant	0,00333	
10	Thermal Softening Exponent	1,03	
11	Melting Temperature	600,61	K
12	Reference Strain Rate (/sec)	1	
13	Shear Modulus	8600	MPa
14	Shock EOS Linear		
19	Johnson Cook Failure		
20	Damage Constant D1	0,25	
21	Damage Constant D2	0	
22	Damage Constant D3	0	
23	Damage Constant D4	0	
24	Damage Constant D5	0	
25	Melting Temperature	327,46	C
26	Reference Strain Rate (/sec)	1	

Properties of Outline Row 4: Ramor500

	A	B	
1	Property	Value	
2	Density	7850	kg m^-3
3	Specific Heat	500	J kg^-1 K^-1
4	Johnson Cook Strength		
5	Strain Rate Correction	First-Order	
6	Initial Yield Stress	1450	MPa
7	Hardening Constant	1288	MPa
8	Hardening Exponent	0,483	
9	Strain Rate Constant	0,02131	
10	Thermal Softening Exponent	0,4505	
11	Melting Temperature	1530	C
12	Reference Strain Rate (/sec)	0,01	
13	Bulk Modulus	1,7008E+05	MPa
14	Shear Modulus	78500	MPa

Figure 6.10 Necessary parameters for Explicit Dynamic Analyze .

Afterwards, we must assign materials to their belonged parts (Figure 6.11).

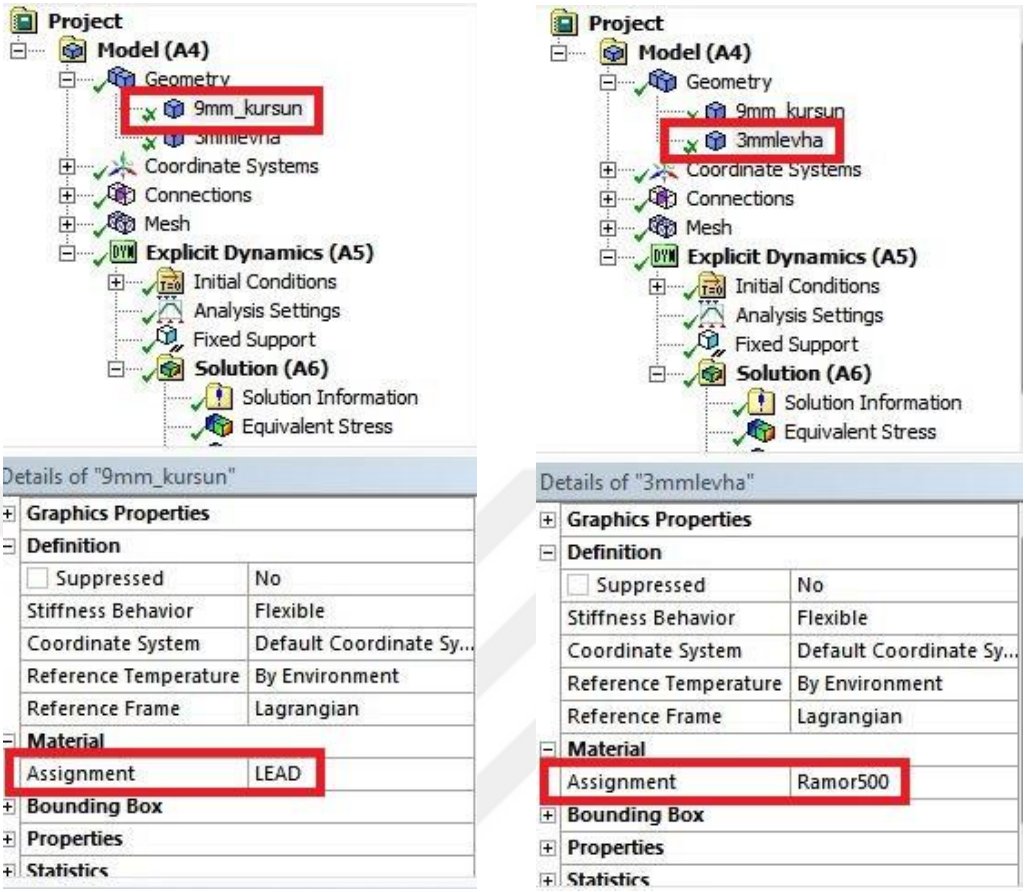

Figure 6.11 Assignment of materials.

Mesh size of the bullet is 0.5 mm and the plate was meshed via “Mapped Face Meshing” (Figure 6.12).

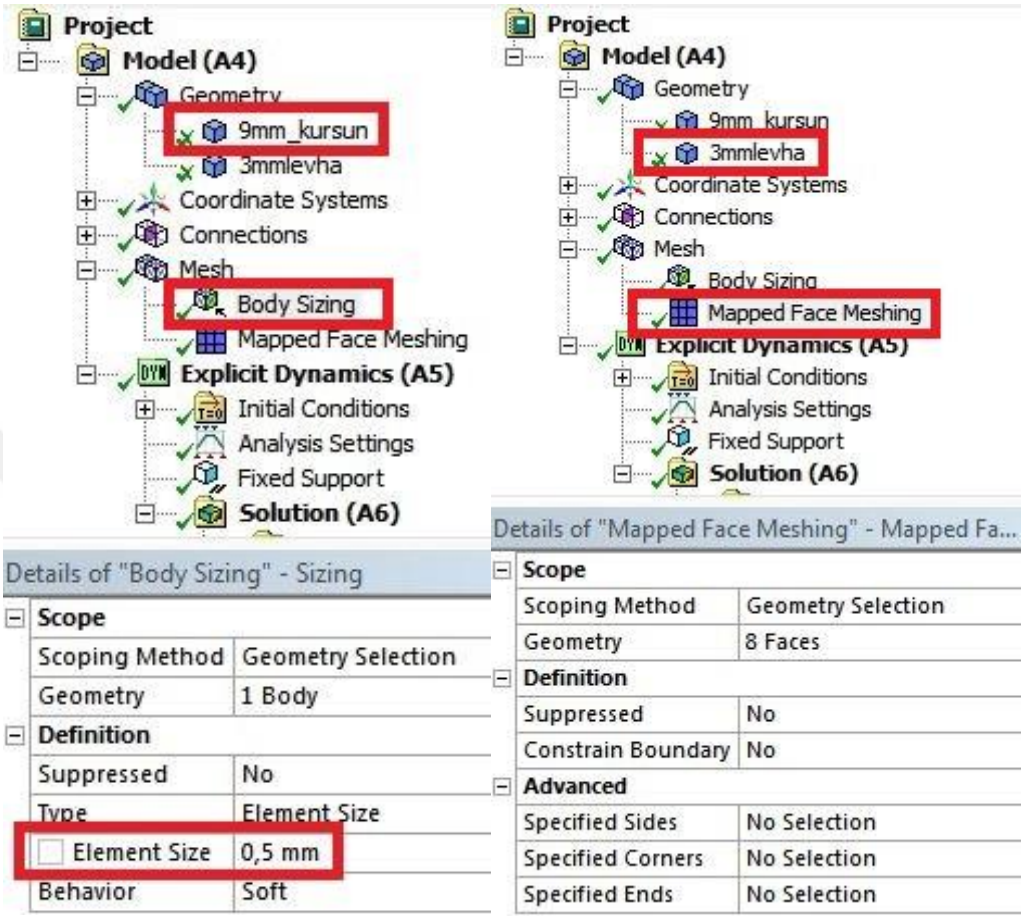

Figure 6.12 Details of meshing.

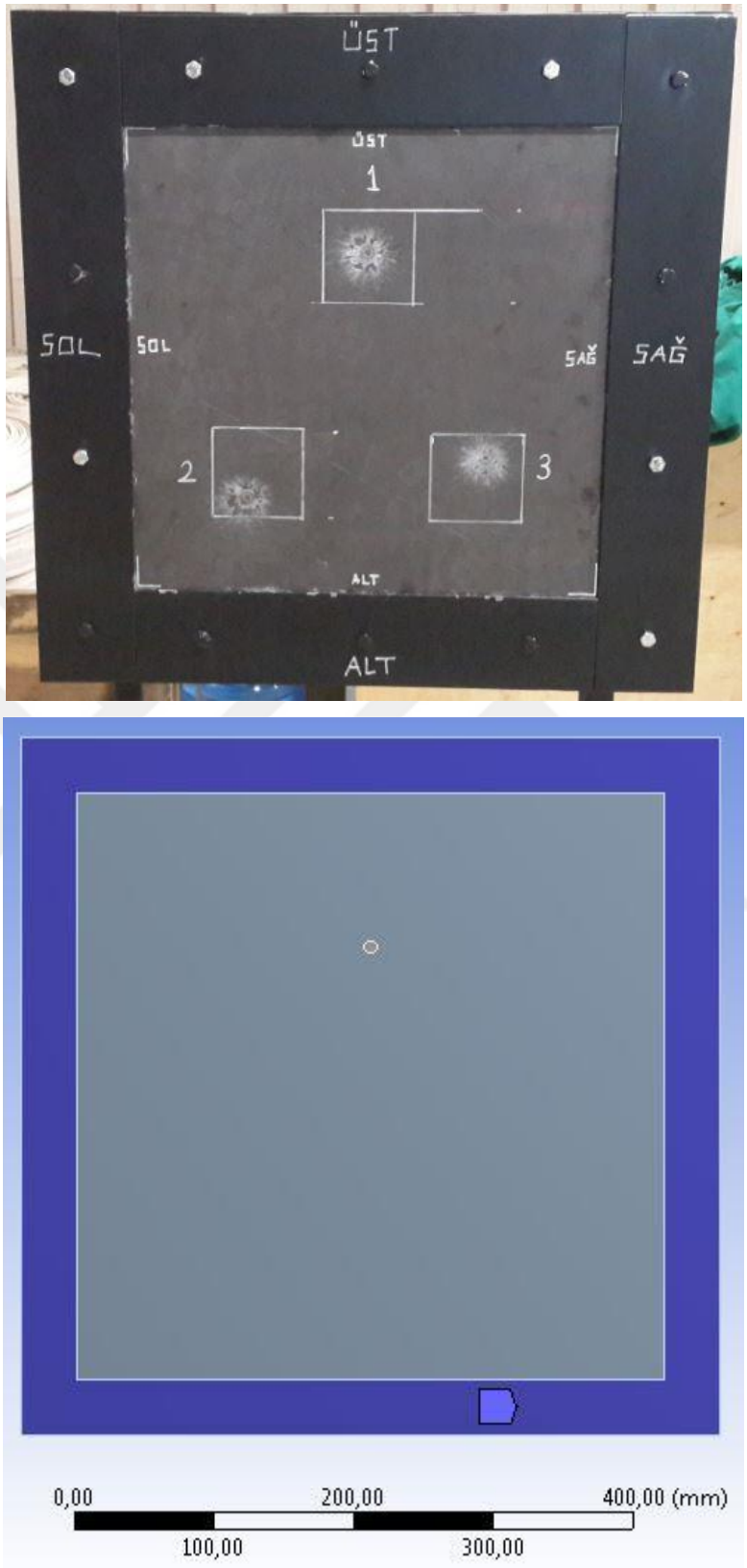

Figure 6.13 Fixing process of the plate.

Velocity of the bullet is 430 m/s, time of analyze is 5.10^{-4} s (Figure 6.14)

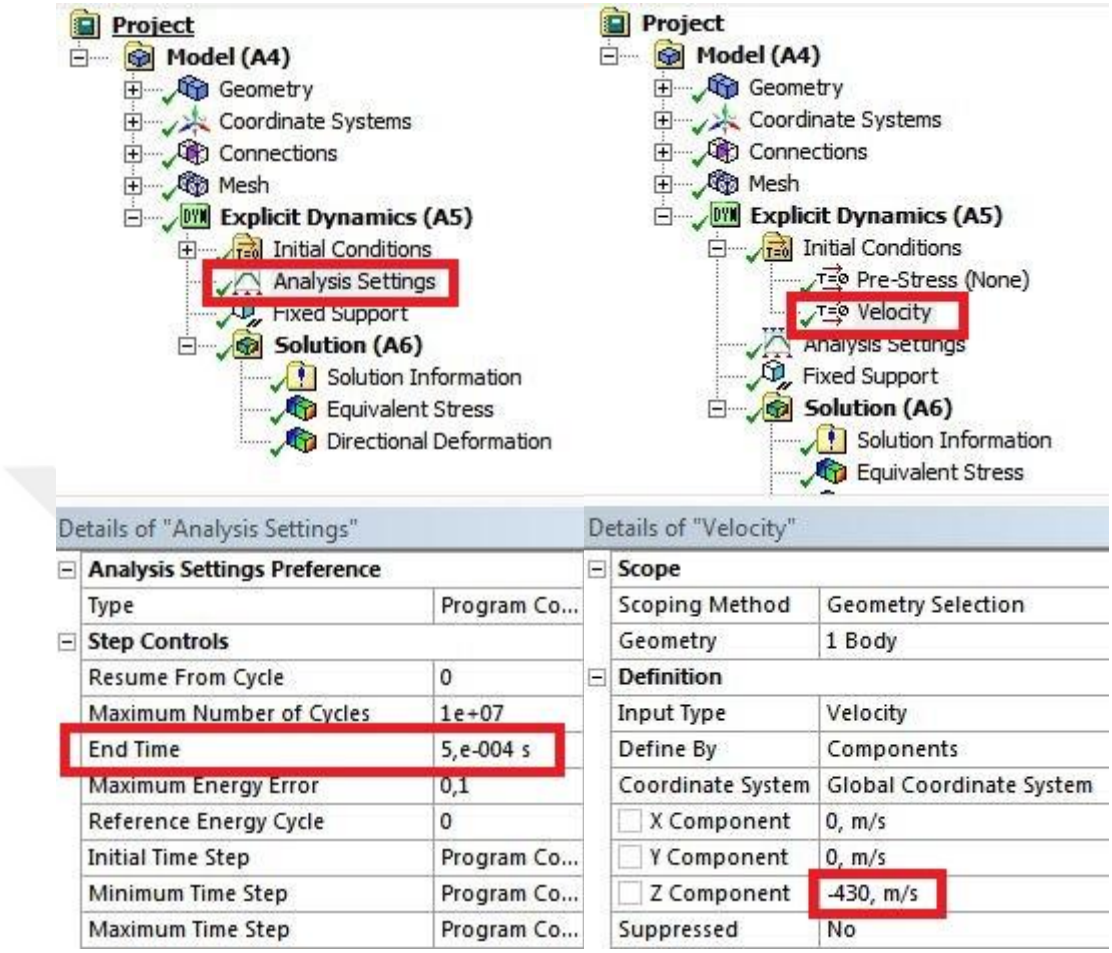

Details of "Analysis Settings"	
Analysis Settings Preference	
Type	Program Co...
Step Controls	
Resume From Cycle	0
Maximum Number of Cycles	1e+07
End Time	5,e-004 s
Maximum Energy Error	0,1
Reference Energy Cycle	0
Initial Time Step	Program Co...
Minimum Time Step	Program Co...
Maximum Time Step	Program Co...

Details of "Velocity"	
Scope	
Scoping Method	Geometry Selection
Geometry	1 Body
Definition	
Input Type	Velocity
Define By	Components
Coordinate System	Global Coordinate System
X Component	0, m/s
Y Component	0, m/s
Z Component	-430, m/s
Suppressed	No

Figure 6.14 End time and velocity.

Finally, some changes were made on the analyze settings (Figure 6.15)

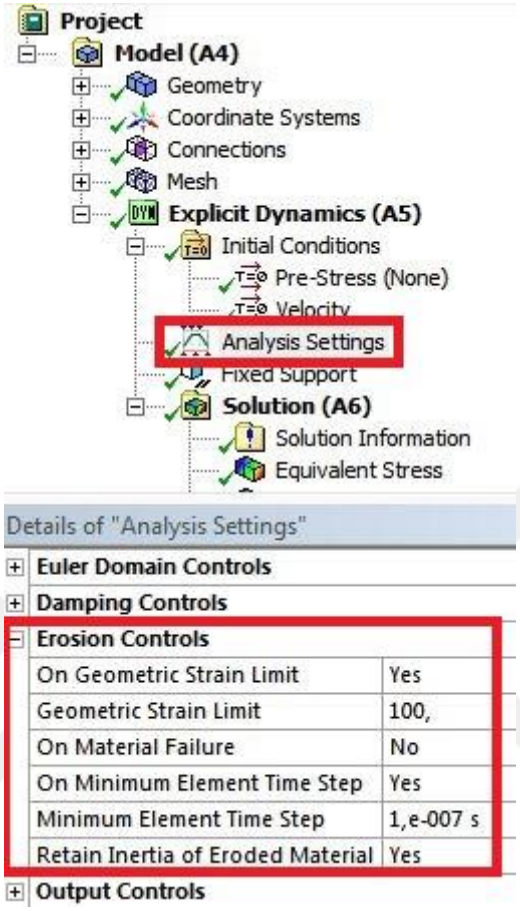

Figure 6.15 Erosion controls settings.

CHAPTER SEVEN
RESULTS AND DISCUSSION

Analysis were repeated for 3 mm, 2.5 mm, 2 mm and 1.5 mm thicknesses and noticed that 1.5 mm thickness is not resistant for 9 mm FMJ bullet at 430 m/s (Figure 7.1, 7.2, 7.3, 7.4)

In Figure 7.1, maximum stress is 473 MPa and maximum displacement is 2.479 mm at 3 mm sheet.

In Figure 7.2, maximum stress is 440 MPa and maximum displacement is 4.272 mm at 2.5 mm sheet.

In Figure 7.3, maximum stress is 580 MPa and maximum displacement is 5.97 mm at 2 mm sheet.

In Figure 7.4, the failure is shown at 1.5 mm sheet and the failure stress is 1717 MPa as shown at the table.

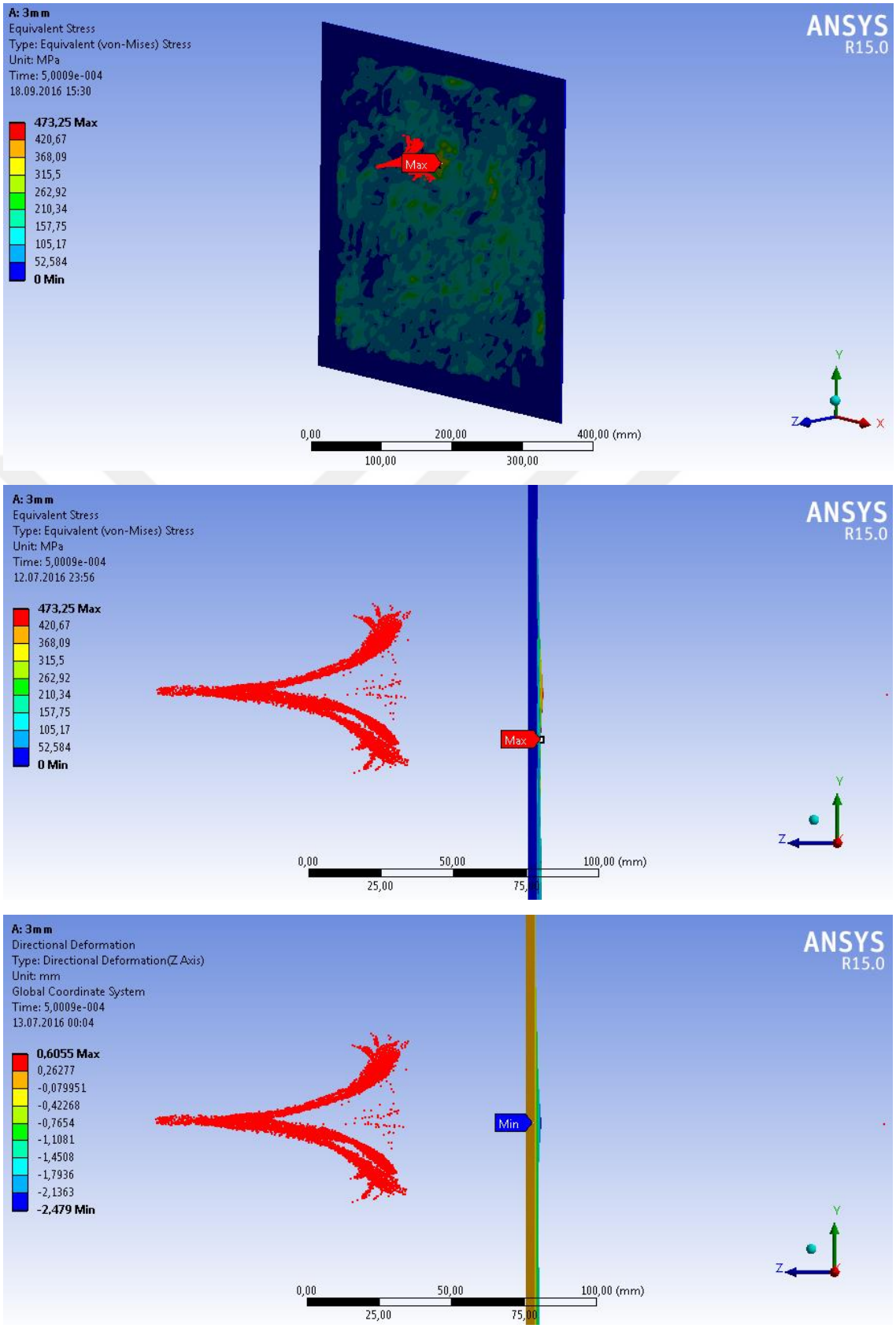

Figure 7.1 Shooting analyze for 3 mm Ramor500.

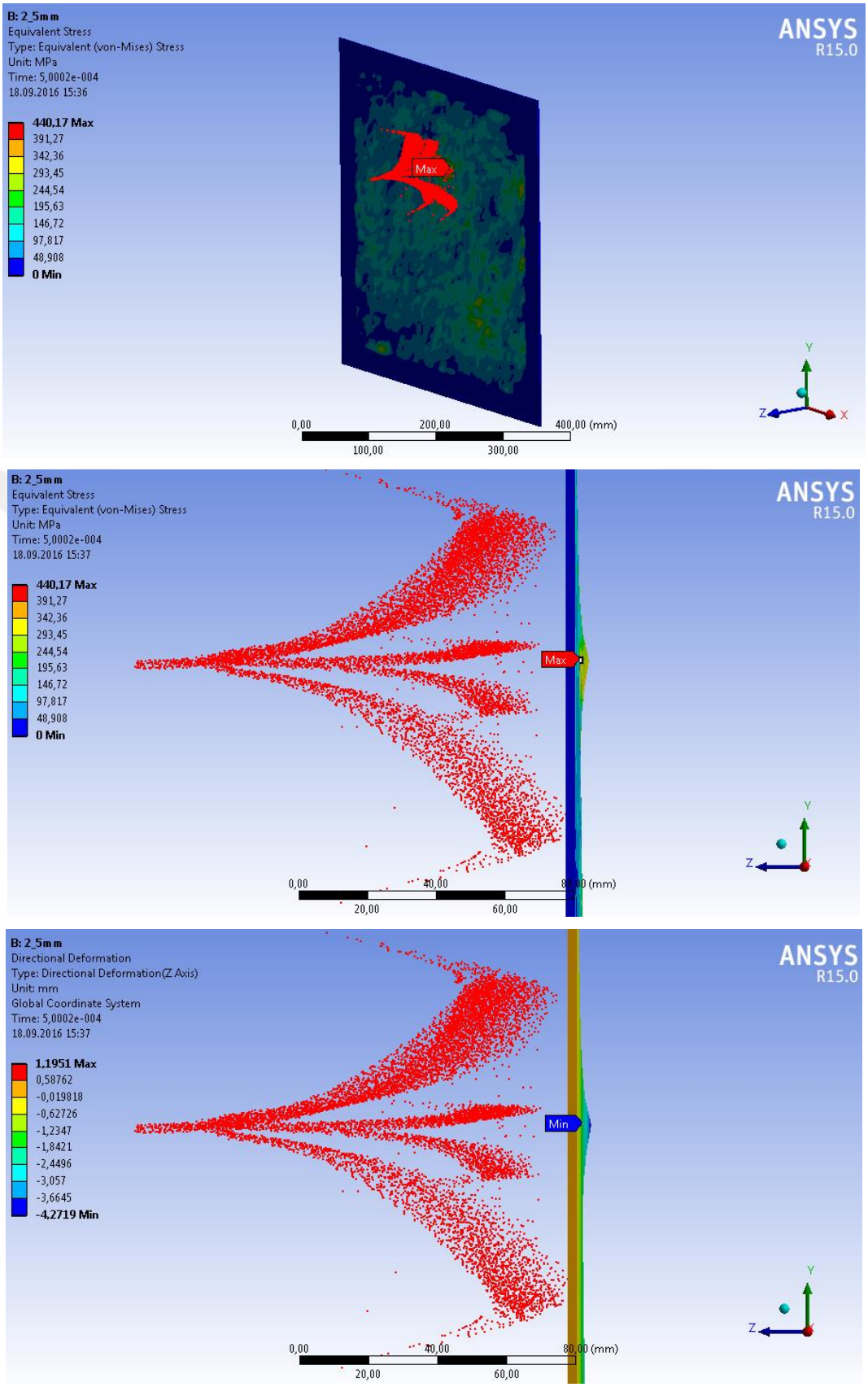

Figure 7.2 Shooting analyze for 2.5 mm Ramor500.

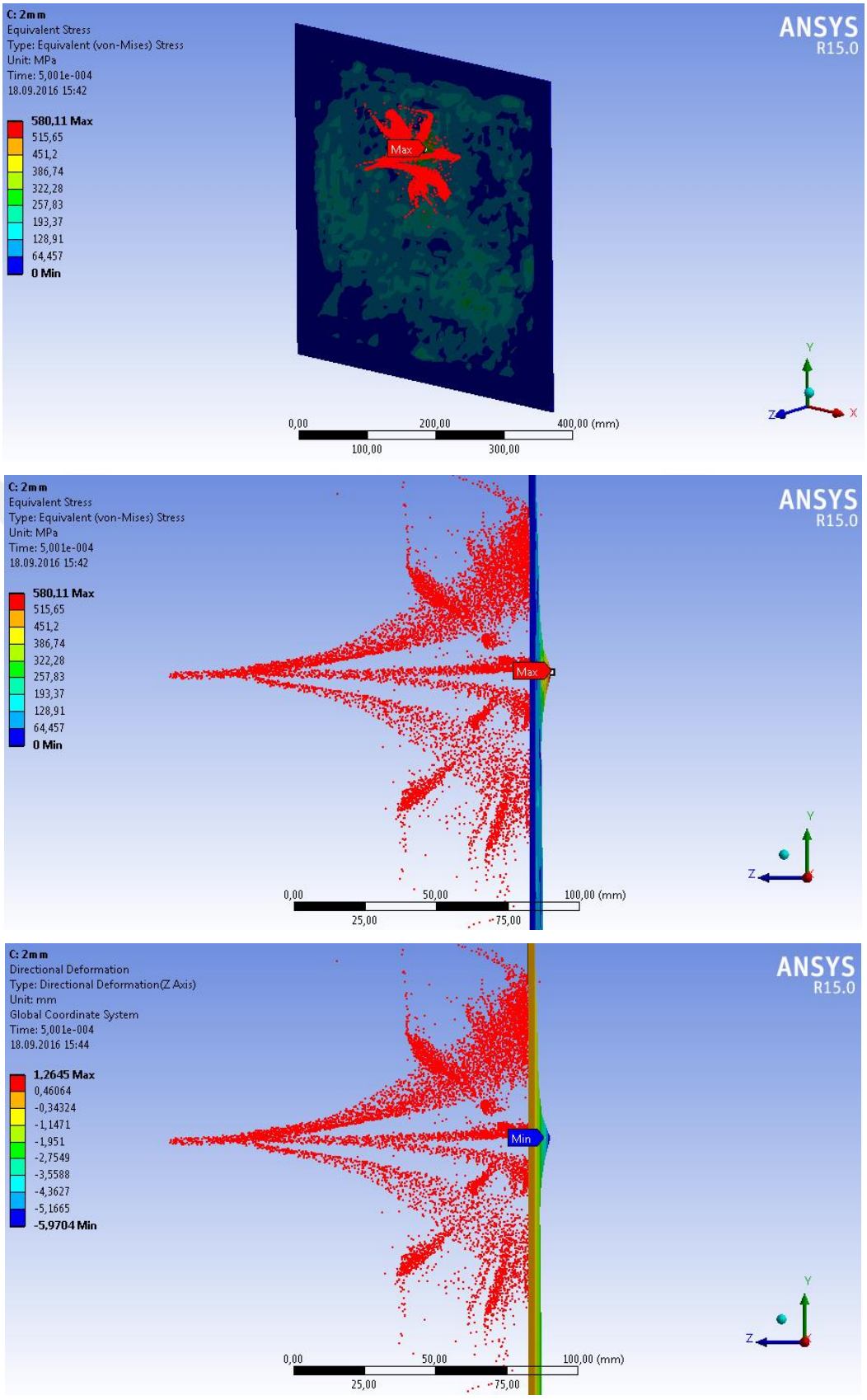

Figure 7.3 Shooting analyze for 2 mm Ramor500.

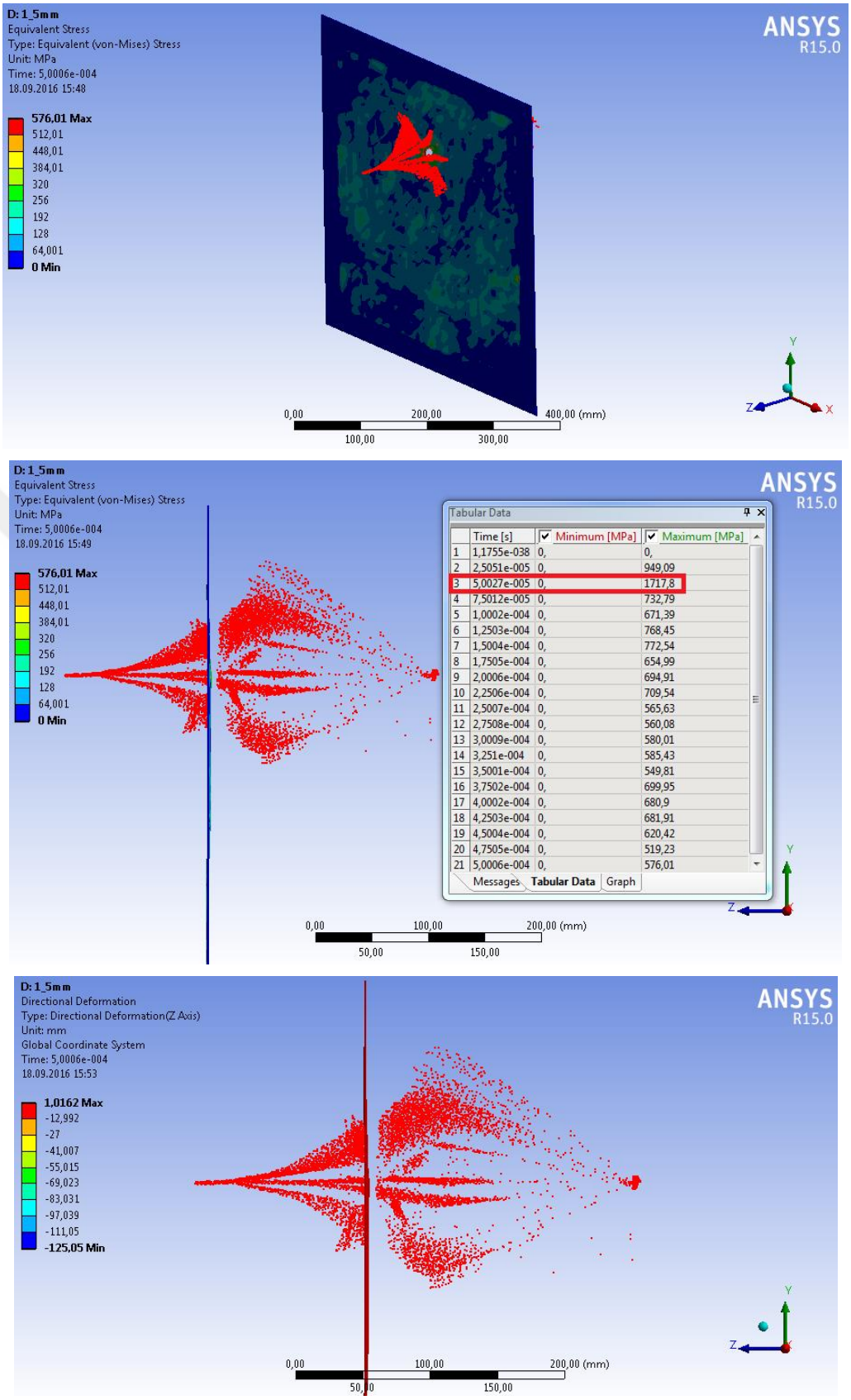

Figure 7.4 Shooting analyze for 1.5 mm Ramor500.

After all shooting test there are no hole on specimens and all displacements are under 44 mm except 1.5 mm thickness sheet.

At the second stage of the study we will try to find out the critical puncture velocity of the bullet on the plate in 3mm thickness.

The original velocity of FMJ bullet is 430 m/s and we have already analyzed the effect of this velocity on Ramor500 armor steel. At the next step we will increase the velocity and repeat the analyze until puncture.

In Figure 7.5, maximum stress is 486 MPa and maximum displacement is 5.5 mm at 550 m/s velocity.

In Figure 7.6 maximum stress is 529.8 MPa and maximum displacement is 6.9 mm at 600 m/s velocity.

In Figure 7.7, maximum stress is 593.6 MPa and maximum displacement is 9.8 mm at 700 m/s velocity.

In Figure 7.8, maximum stress is 694.5 MPa and maximum displacement is 13.5 mm at 800 m/s velocity. The material is unstable at this velocity.

In figure 7.9, the failure is shown at 900 m/s.

After all shooting test there are no hole on specimens and all displacements are under 44 mm except shooting 900 m/s.

Figure 7.5 shows the stress and distribution of bullet at 550 m/s.

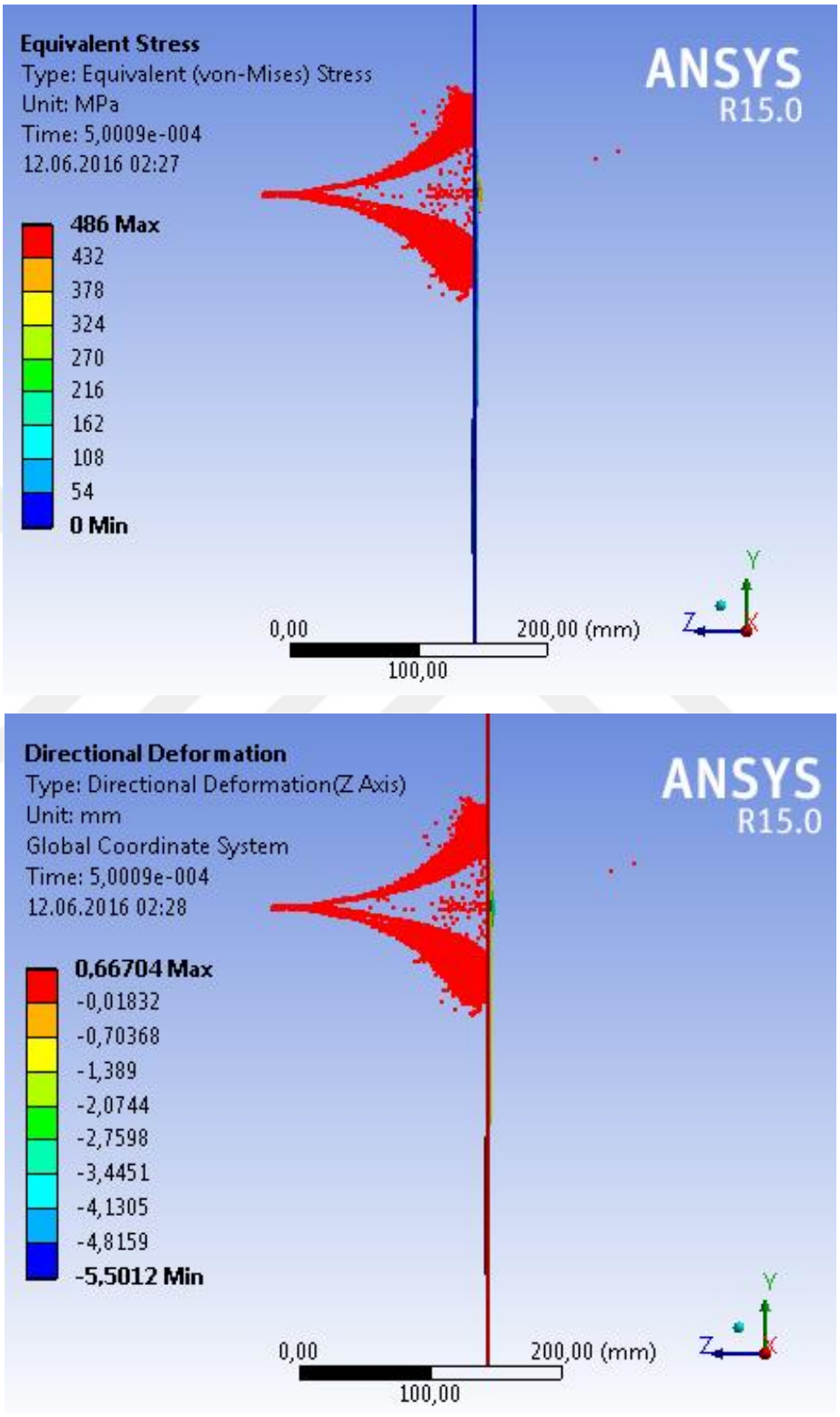

Figure 7.5 Stress and distribution at 550 m/s.

Figure 7.6 shows the stress and distribution of bullet at 600 m/s.

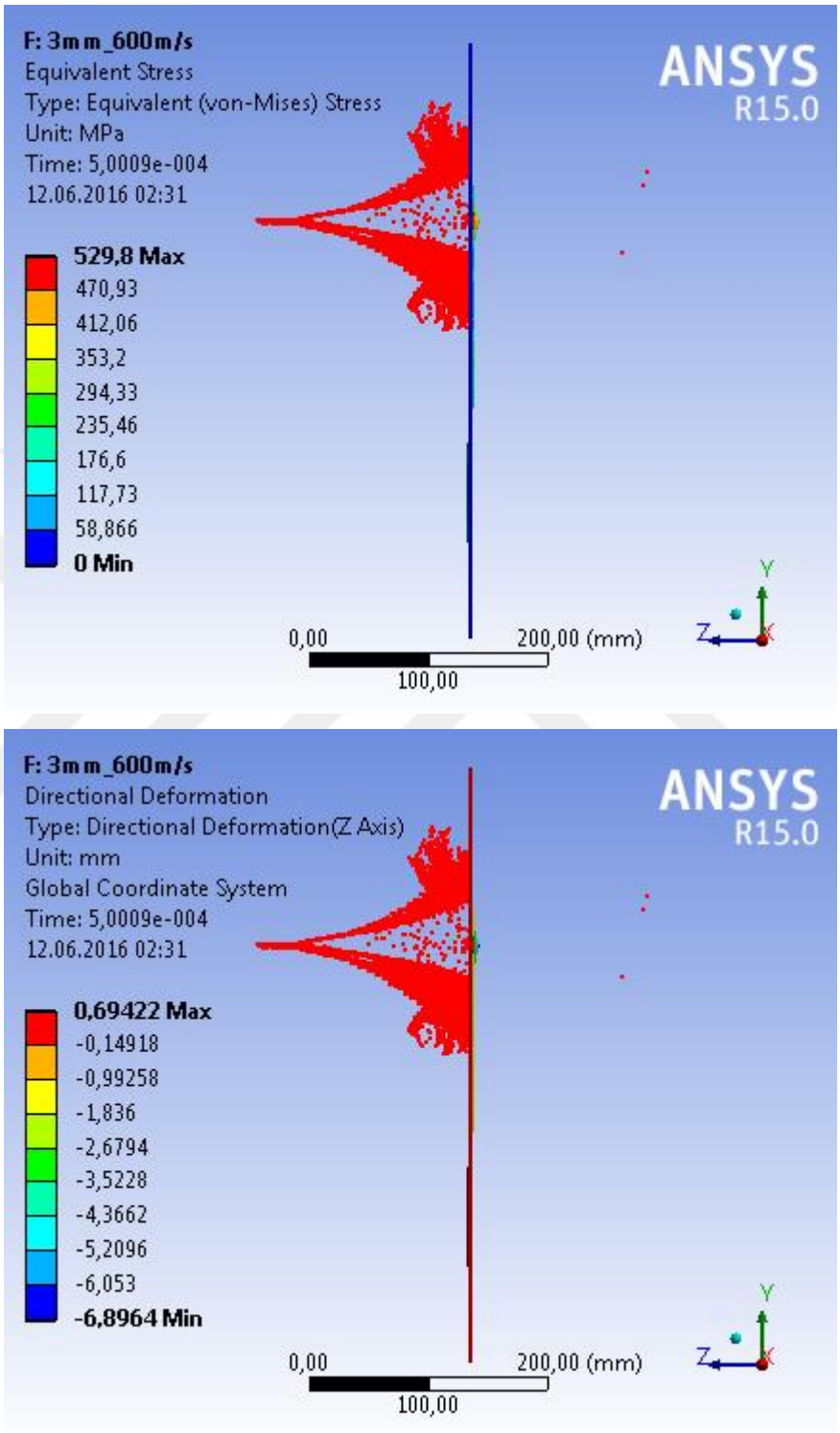

Figure 7.6 Stress and distribution at 600 m/s.

Figure 7.7 shows the stress and distribution of bullet at 700 m/s.

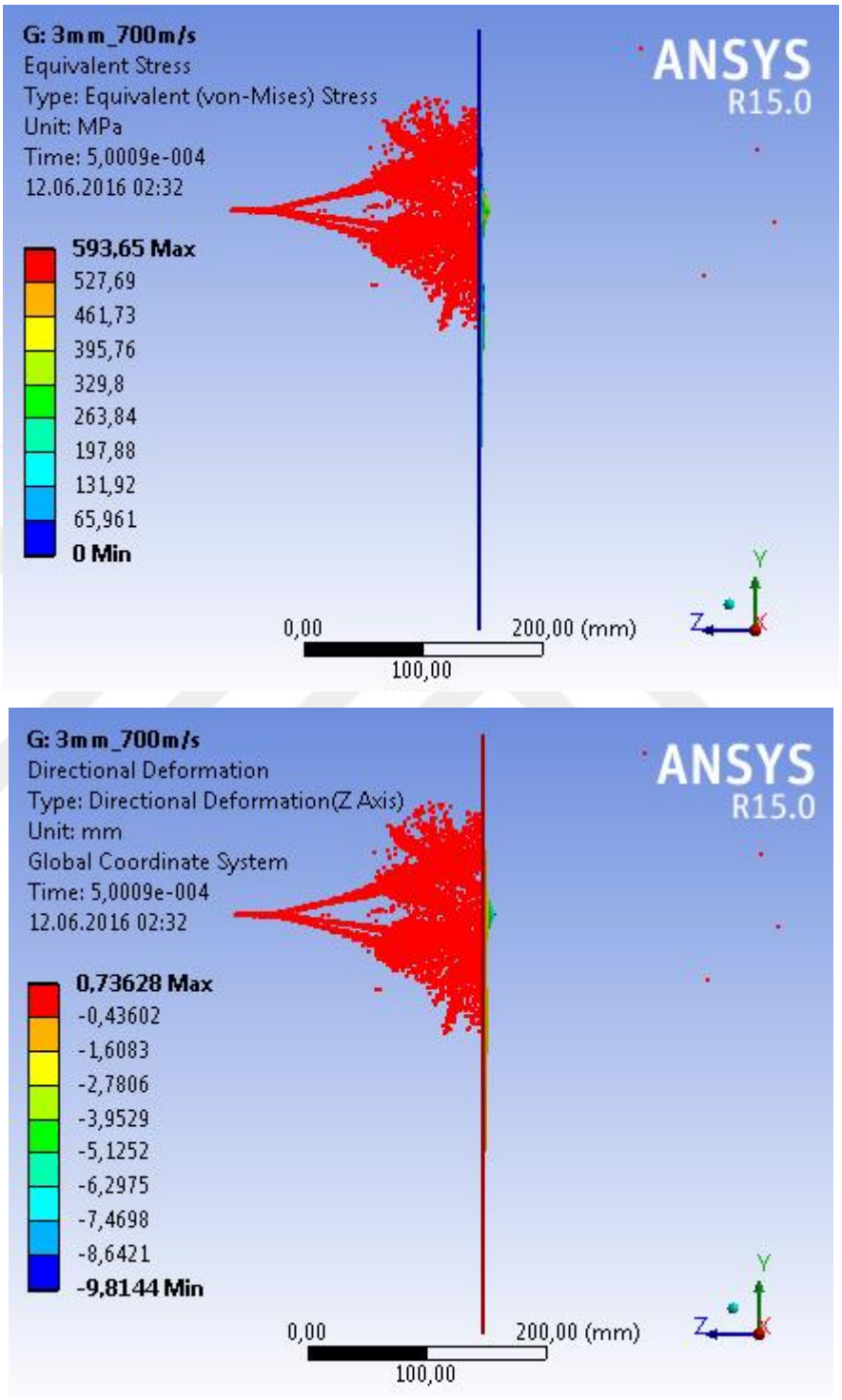

Figure 7.7 Stress and distribution at 700 m/s.

Figure 7.8 shows the stress and distribution of bullet at 800 m/s.

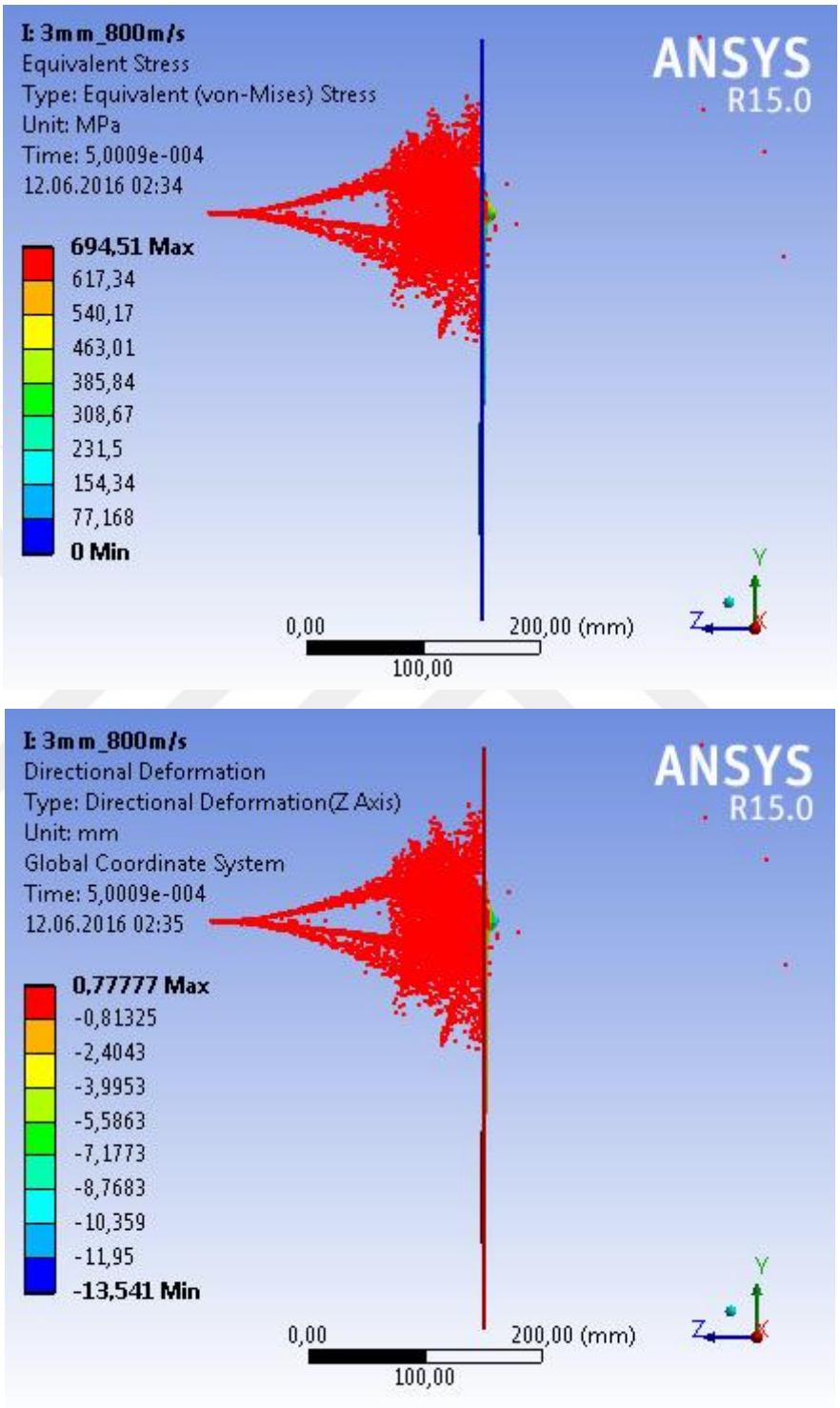

Figure 7.8 Stress and distribution at 800 m/s.

Figure 7.9 shows the stress and distribution of bullet at 900 m/s.

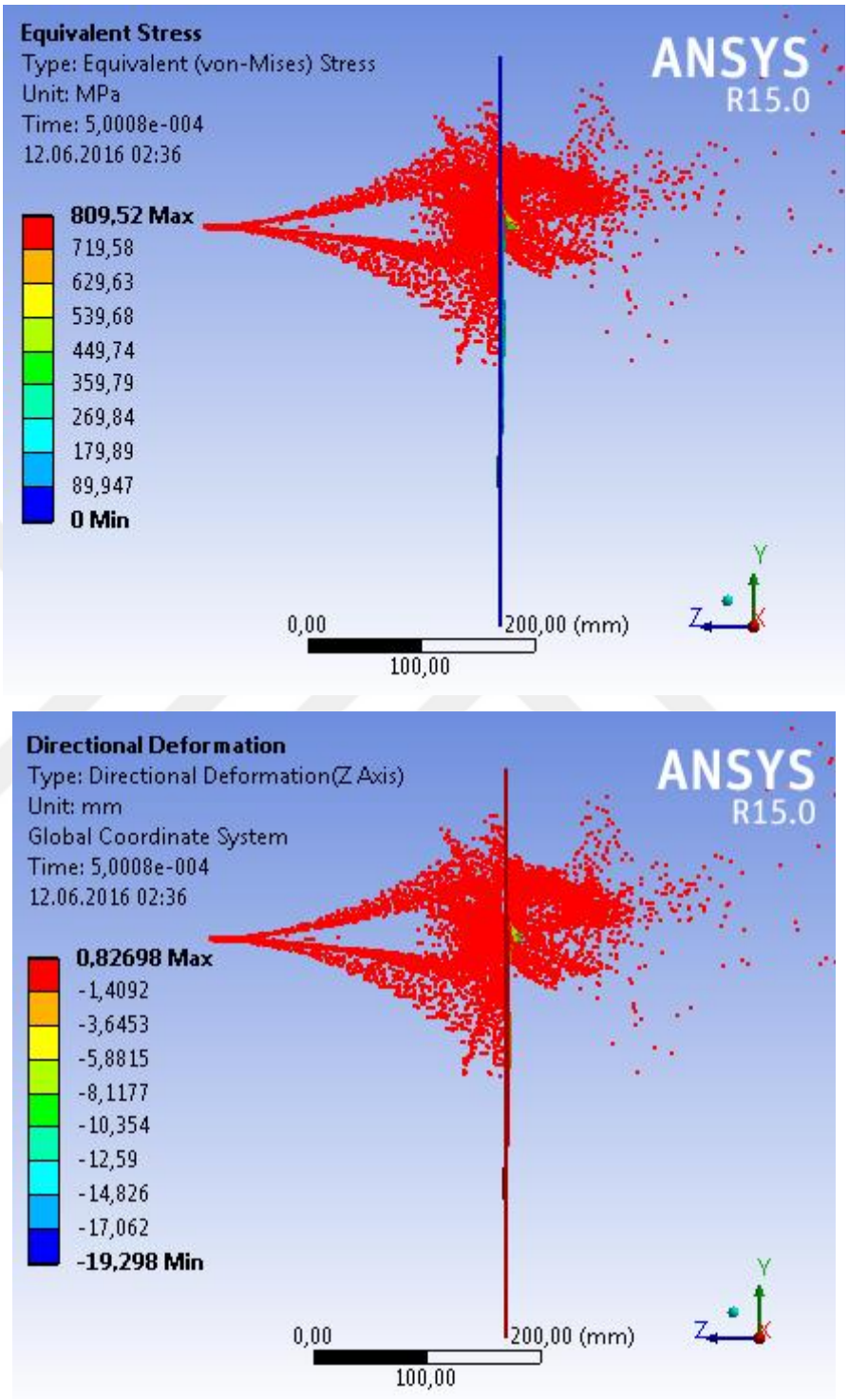

Figure 7.9 Stress and distribution at 900 m/s.

The stress-velocity graph is given at Figure 7.10

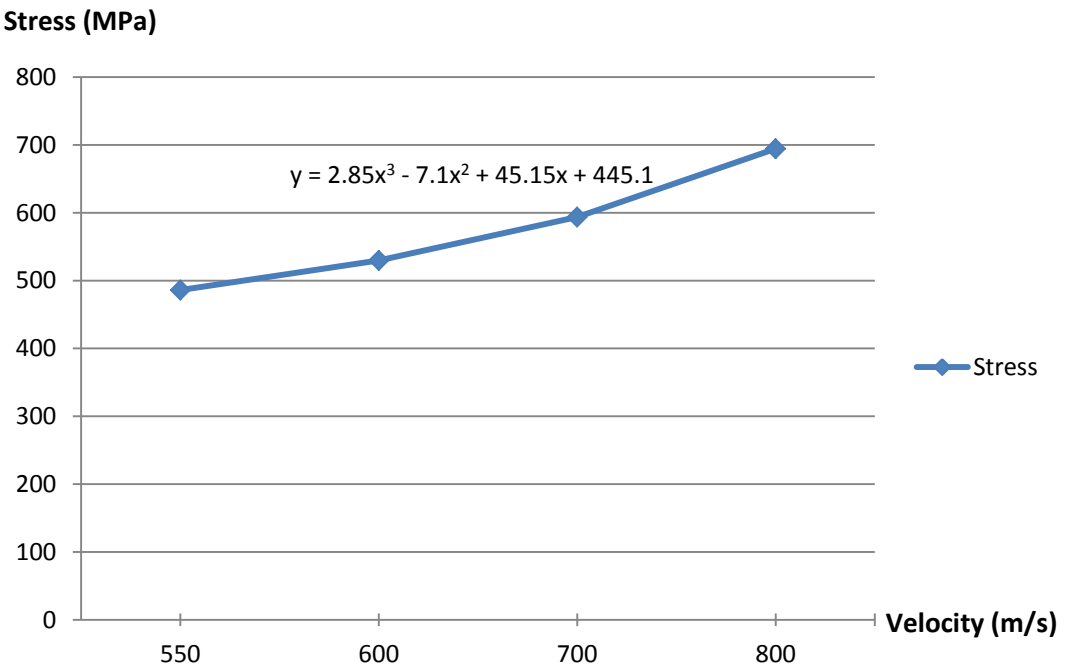

Figure 7.10 Stress-velocity graph of Ramor500.

According to the graph, the relation between stress and velocity is not linear. Instability is increasing polynomial.

CHAPTER EIGHT
CONCLUSION

Aftter experimental and numerical studies, the results are below:

1- It is realised that experimental and numerical results are concordant each other. That's why it is prouded that realistic results could be obtained via numerical simulation instead of expensive experimental studies.
2- At the first stage of the study, 9 mm FMJ bullets were shot to different specimens which have different thickness. All specimens has displacement under 44 mm and no hole or crack except 1.5 mm specimen. The minimum thickness of Ramor500 armor steel was determined 1.5 mm for NIJ LEVEL IIIA.
3- At the second stage of the study, 9 mm FMJ bullets at different velocities were shot to specimens which have 3 mm thickness. All specimens has displacement under 44 mm and no hole or crack except 900 m/s velocity. The minimum puncture velocity of 9 mm FMJ projectile was determined 900 m/s for Ramor500 in 3 mm thickness.

After the experimental study, the bullet is shown at Figure 5.10, the specimen is shown at Figure 6.13.

All tests show us Ramor500 armor steel in 3 mm thickness is suitable for NIJ LEVEL IIIA.

REFERENCES

Abaqus Technology Brief (2012). *Simulation of the ballistic perforation of aluminum plates with Abaqus/Explicit*. Retrieved October 5, 2015, from *http://www.3ds.com/fileadmin/PRODUCTS/SIMULIA/PDF/tech-briefs/aero-ballistic-perforation-alumnium-plates-12.pdf.*

Balistik nedir, (n.d.). Retrieved June 12, 2016, from http://www.adlibilimler.net/content/balistik-nedir.

Bhat, A. R. (2007). *Finite element modeling and dynamic impact response evaluation for ballistic applications.* M.Sc Thesis, Mumbia University, India.

Bullet, (n.d.). Retrieved July 7, 2016, from https://en.wikipedia.org/wiki/Bullet.

Candan, C. (2007). *Hafif silahlara karşı preslenerek ve preslenmeden üretilen yüksek yoğunluklu polietilen (UHMW-PE) zırh plakalarının termina balistik özelliklerinin incelenmesi.* Retrieved February 27, 2014, from *http://www.endil.yildiz.edu.tr/proceedings/18.pdf*

Demircioğlu, T. K., Candan, C., & Ay, İ. (2011). *Organik matrisli kompozit malzeme kullanılarak oluşturulan hibrit zırh plakasının terminal balistik özelliklerinin incelenmesi.* Retrieved February 27, 2014, from http://w3.balikesir.edu.tr/~ay/communiques/bildiri16.pdf

Engineering, (n.d.). Retrieved August 10, 2016, from http://www.cpdlr.com/notes-articles-engineering/239-explicit-dynamics-by-using-ansys.html.

Flanging, raex wear resistant steels, ultra high strength optim qc steels, (n.d.). Retrieved June 25, 2016, from http://docslide.us/documents/ruukki-hot-rolled-steels processing-of-material-flanging-raex-and-optim-qc.html.

Hot rolled steel sheets, plates and coils mechanical cutting, (n.d.). Retrieved July 3, 2016, from http://docslide.us/documents/ruukki-hot-rolled-steels-processing-of-material-mechanical-cutting.html.

Karagöz, Ş., & Atapek, H. (2007). Bor yakıtlı zırh çeliklerinin kırılma davranışı. *Prooceedings of 8th International Fracture Conference.*

Kıranlı, E. (2009). *Determination of material constitutive equation of a biomedical grade Ti6Al4V alloy for cross-wedge rolling.* M.Sc Thesis, İzmir Institute of Technology, Turkey.

Machining, (n.d.). Retrieved July 3, 2016, from http://www.ruukki.fr/~/media/Files/Steel-products/Hot-rolled-steels- processing instructions/Ruukki-Hot-rolled-steels-Processing-of-material-Machining.pdf.

National Institute of Standards and Technology (2008*). Ballistic resistance of body armor NIJ Standard–0101.06.* Retrieved April 23, 2014, from https://www.ncjrs.gov/pdffiles1/nij/223054.pdf .

Proulx, T. (Ed.). (2011). Experimental and applied mechanics, Volume 6. *Proceedings of the 2011 Annual Conference on Experimental and Applied Mechanics.*

Quan, X., Birnbaum, N. K., Cowler, M. S., & Gerber, B. I. (2003). *Numerical simulation of structural deformation under shock and impact loads using a coupled multi-solver approach.* Retrieved June 12, 2016, from *http://truegrid.com/paper152.pdf*

Ramor protection steels for the advanged safety of life and property, (n.d.). Retrieved June 15, 2016, from http://www.ruukki.fr/~/media/Files/Steel-products/Hot-rolled-steels-processing-instructions/Ruukki-Ramor-protection-steels-hand-out-2014.pdf.

Ramor Protection Steels (2016). Retrieved June 10, 2016, from *http://www.oxycoupage.com/FichiersPDF/Ssab/English/Ramor/702-en-SSAB-Ramor-protection-steels.pdf*

Ramor protection steels, (n.d.). Retrieved June 20, 2016, from http://ssabwebsitecdn.azureedge.net.

Ramor zırh çeliği, (n.d.). Retrieved June 16, 2016, from www.ruukki.com.tr.

Shrot, A., & Bäker, M. (2011). *Determination of Johnson–Cook parameters from machining simulations.* Retrieved August 23, 2015, from http://www.sciencedirect.com/science/article/pii/S0927025611004277.

Šlais, M., Dohnal, I., & Forejt, M. (2012). *Determination of Johnson-Cook equation parameters.* Retrieved August 7, 2015, from http://www.ams.tuke.sk/index.php?mi=06&sm=15&nm=2&at=10&lng=sk^# 15210.

TS EN ISO 6892-1 (March 2011). *Metallic materials - Tensile testing - Part 1: Method of test at room temperature*

Ürünlerimiz, *Katmerciler Araç Üstü Ekipman Sanayi ve Ticaret A. Ş.*, (n.d.). Retrieved June 12, 2016, from http://www.katmerciler.com.tr/L/TR/mid/343/g/0/c/31/id/21/Toplumsal-Olaylara-Mudahale-Araci-(TOMA).htm.